Published in final edited form as:

J Neurochem. 2021 February ; 156(4): 445–464. doi:10.1111/jnc.15152.

Glycogen synthase kinase-3ß supports serotonin transporter function and trafficking in a phosphorylation-dependent manner

Durairaj Ragu Varman[1], **Lankupalle D. Jayanthi**[1], **Sammanda Ramamoorthy**[1,*]

[1]Department of Pharmacology and Toxicology, Virginia Commonwealth University, Richmond VA 23298, USA

Abstract

Serotonin (5-HT) transporter (SERT) plays a crucial role in serotonergic transmission in the central nervous system, and any aberration causes serious mental illnesses. Nevertheless, the cellular mechanisms that regulate SERT function and trafficking are not entirely understood. Growing evidence suggests that several protein kinases act as modulators. Here we delineate the molecular mechanisms by which glycogen synthase kinase-3ß (GSK3ß) regulates SERT. When mouse striatal synaptosomes were treated with the GSK3α/ß inhibitor CHIR99021, we observed a significant increase in SERT function, V_{max}, surface expression with a reduction in 5-HT K_m and SERT phosphorylation. To further study how the SERT molecule is affected by GSK3α/ß, we used HEK-293 cells as a heterologous expression system. As in striatal synaptosomes, CHIR99021 treatment of cells expressing wild-type hSERT (hSERT-WT) resulted in a time and dose-dependent elevation of hSERT function with a concomitant increase in the V_{max} and surface transporters due to reduced internalization and enhanced membrane insertion; silencing GSK3α/ß in these cells with siRNA also similarly affected hSERT. Converting putative GSK3α/ß phosphorylation site serine at position 48 to alanine in hSERT (hSERT-S48A) completely abrogated the effects of both the inhibitor CHIR99021 and GSK3α/ß siRNA. Substantiating these findings, overexpression of constitutively active GSK3ß with hSERT-WT, but not with hSERT-

*To whom correspondence should be addressed: Sammanda Ramamoorthy, Department of Pharmacology and Toxicology, Virginia Commonwealth University, Richmond VA 23298; sramamoorthy@vcu.edu or sammanda.ramamoorthy@vcuhealth.org; Tel. (804) 828-8407; Fax. (804) 828-211.

--Human subjects --
Involves human subjects:
If yes: Informed consent & ethics approval achieved:
=> if yes, please ensure that the info "Informed consent was achieved for all subjects, and the experiments were approved by the local ethics committee." is included in the Methods.
ARRIVE guidelines have been followed:
Yes
=> if it is a Review or Editorial, skip complete sentence => if No, include a statement in the "Conflict of interest disclosure" section:
"ARRIVE guidelines were not followed for the following reason:
"
(edit phrasing to form a complete sentence as necessary).
=> if Yes, insert in the "Conflict of interest disclosure" section:
"All experiments were conducted in compliance with the ARRIVE guidelines." unless it is a Review or Editorial

CONFLICT OF INTEREST
The authors declare no conflict of interest.

OPEN SCIENCE BADGES
This article has received a badge for *Open Materials* because it provided all relevant information to reproduce the study in the manuscript. More information about the Open Science badges can be found at https://cos.io/our-services/open-science-badges/

S48A, reduced SERT function, V_{max}, surface density, and enhanced transporter phosphorylation. Both hSERT-WT and hSERT-S48A were inhibited similarly by PKC activation or by inhibition of Akt, CaMKII, p38 MAPK or Src kinase. These findings provide new evidence that GSK3ß supports basal SERT function and trafficking via serine-48 phosphorylation.

Keywords

serotonin transporter; serotonergic transmission; uptake; glycogen synthase kinase-3; trafficking; phosphorylation

INTRODUCTION

Serotonin or 5-hydroxytryptamine (5-HT) is known to affect many neurophysiological processes and behavior (Fozzard 1989, Jacobs & Azmitia 1992). In serotonergic neurotransmission, the reuptake of released 5-HT by Na^+/Cl^--dependent serotonin transporter (SERT) is an important process (Ramamoorthy et al. 1993, Bengel et al. 1998). SERT polymorphisms in the promoter and introns, and rare and rare functional coding variants in the exons are linked to various types of psychopathology (Hahn & Blakely 2007, Murphy & Moya 2011, Cook et al. 1997, Murphy et al. 2004). SERT blockers such as selective serotonin reuptake inhibitors (SSRIs) are effective clinical antidepressants and anxiolytics (Kent et al. 1998, Ballenger 1999, Kugaya et al. 2003). GSK3β modulates neuronal plasticity (Frame & Cohen 2001, Grimes & Jope 2001). Impaired serotonergic activity has long been associated with depression (Berger et al. 2009, Owens & Nemeroff 1994). Hyperactive GSK3β knock-in mice have heightened learned helplessness, an accepted model of depression-like behavior (Pardo et al. 2016). Thus, there is an intricate relationship between GSK3β activity and serotonergic system including SERT activity.

The functional expression of SERT is dynamically regulated by several kinases and receptors (Rajamanickam et al. 2015, Annamalai et al. 2012, Samuvel et al. 2005, Jayanthi et al. 2005, Jayanthi et al. 1994, Zhu et al. 2005, Ramamoorthy et al. 2007, Miller & Hoffman 1994, Reviewed Ramamoorthy et al. 2011, Bermingham & Blakely 2016). We have demonstrated that SERT is a phosphoprotein and is constitutively phosphorylated (Ramamoorthy et al. 2011). SERT basal phosphorylation is sensitive to p38 MAPK and Akt inhibition (Samuvel et al. 2005, Rajamanickam et al. 2015). Signaling pathways involving PKC, CaMKII, p38 MAPK, Akt, PKA, Src, and PKG also regulate SERT phosphorylation (Rajamanickam et al. 2015, Annamalai et al. 2012, Ramamoorthy et al. 2007, Samuvel et al. 2005, Jayanthi et al. 2005, Ramamoorthy et al. 1998). Furthermore, SERT substrates and inhibitors impact kinase-mediated SERT regulation. (Ramamoorthy & Blakely 1999).

In a cell, GSK3 is usually constitutively active, and its canonical site of phosphorylation is S/T-X-X-X-S/T(P) (Ubersax & Ferrell 2007, Doble & Woodgett 2003). The presence of serine 44 (S44) and serine 48 (S48) within the cytoplasmic N-terminus of SERT represents this motif. However, whether this SERT motif is a site of phosphorylation for GSK3α/ß and whether GSK3α/ß-mediated SERT phosphorylation plays a role in SERT regulation are yet to be demonstrated. In this study, we identify GSK3α/ß phosphorylation site in the SERT, and provide evidence for GSK3β-mediated SERT phosphorylation playing a role in

sustaining the basal function and trafficking of SERT in native neuronal tissue and a heterologous cell model.

MATERIALS AND METHODS

Materials

All reagents and chemicals were purchased within 2 years and stored according to manufacturer's instructions. Cell culture media DMEM (Dulbecco's modified Eagle's medium; (Gibco, Cat # 11885-084) and Lipofectamine™ 2000 (Cat# 11668-019) were purchased from Invitrogen/Life science Technologies (Grand Island, NY). Fetal bovine serum (Cat# 10437-028) was obtained from Hyclone/GE Healthcare Life Sciences (Logan, UT). CHIR99021 ((6-[2-([4-(2,4-dichlorophenyl)-5-(5-methyl-1H-imidazol-2-yl)-2pyrimidinyl) aminoethyl) amino]-3-pyridinecarbonitrile)) (Cat# 361559, Millipore), 2-mercaptoethanesulfonate (MesNa) (Cat# M1511), serotonin hydrochloride (Cat# H9523), ß-PMA (phorbol-12,13-dibutyrate) (Cat# 524390-Calbiochem), PD169316 (4-(4-Fluorophenyl)-2-(4-nitrophenyl)-5-(4-pyridyl)-1H-imidazole) (Cat# 513030-Calbiochem), KN-93 (2-[N-(2-hydroxyethyl)]-N-(4-methoxybenzenesulfonyl)]amino-N-(4-chlorocinnamyl)-N-methylbenzylamine) (Cat# 422708-Calbiochem), PP2 (4-Amino-5-(4-chlorophenyl)-7-(*t*-butyl)pyrazolo[3,4-d]pyrimidine) (Cat# 529573-Calbiochem), Akt-X (10-(4′-(N-diethylamino)butyl)-2-chlorophenoxazine) (Cat# 124020-Calbiochem), protease (Cat# P8340) and phosphatase inhibitor (Cat# P0044) cocktails were obtained from Sigma-Aldrich (St. Louis, MO). 5-Hydroxy-(^{3}H) tryptamine creatine sulphate (Cat# NET498001MC), $^{32}PO_4$ carrier free orthophosphate and Optiphase Supermix were obtained from PerkinElmer Inc and Analytical Sciences (Waltham, MA). SDS/PAGE reagents and Bradford protein assay (Cat# 5000006) were purchased from Bio-Rad (Hercules, CA), ECL reagents-Supersignal West pico chemiluminescent substrate (Cat# 34580), transferrin receptor antibody H68.4 (RRID: AB-2533029) were purchased from Thermo Fischer Scientific Inc., (Rockford IL). HyBlot CL autoradiography films (Cat# E3012) was purchased from Thomas Scientific (Swedesboro, NJ). Protein A sepharose beads (Cat# 17-0780-01) was obtained from GE Healthcare Life Sciences (Pittsburg PA), EZ link NHS-Sulfo-SS-biotin (Sulfosuccinimidyl-s-[biotinamido]ethyi-1.3-dithiopropionate) (Cat# 21331) and NeutrAvidin Agarose Beads (Cat# 29201) were purchased from Pierce (Rockford, IL). The Quickchange site-directed mutagenesis kit (Cat# 200521-5) was from Agilent (Santa Clara, CA). Rabbit polyclonal anti-SERT (SR-12) were generated by our laboratory and their specificity were thoroughly characterized in our previous studies and published (Sundaramurthy et al. 2017, Rajamanickam et al. 2015, Annamalai et al. 2012, Ramamoorthy et al. 2007, Jayanthi et al. 2005, Samuvel et al. 2005). SERT-SR-12 will be shared upon reasonable request. Anti-calnexin antibody (RRID: AB-312058) was from Enzo Life Sciences, Inc (Farmingdale, NY). The HRP-conjugated antibodies (RRID: AB-2313561, RRID: AB-10015289) were from Jackson ImmunoResearch Laboratories (West Grove, PA). All HA-GSK3ß-constructs (RRID: Addgene-14753 (HA GSK3ß WT), RRID: Addgene-14754 (HA GSK3ß S9A), RRID: Addgene-14755 (HA GSK3ß K85A) (deposited by Dr. Jim Woodgett) were obtained from Addgene (Watertown, MA). RRID: Addgene-15483 (hSERT pcDNA3) and pcDNA3.1 (Cat# V790-20, Invitrogen, Inc.). GSK-3 antibody sampler kit (Cat# 9369, RRID: AB-2636978 (GSK3ß), RRID: AB-2798445

(p(S9)-GSK3ß)) was from Cell Signaling Technology (Danvers, MA). On-TARGETplus human GSK3α/ß siRNA-SMARTpool was purchased from horizon-Dharmacon (Lafaytte, CO). All other chemicals were obtained from Sigma-Aldrich (St. Louis, MO) or Fisher Scientific (Waltham, MA) unless otherwise indicated.

Animals

All animal procedures were followed in accordance with the National Institutes of Health's *Guide for the Care and Use of Laboratory Animals* and approved by Institutional Animal Care and Use Committee at Virginia Commonwealth University (approved protocol number AD10000476). Male adult C57BL/6 mice (The Jackson Laboratory, RRID: IMSR-JAX:000664) of 25-30 g body weight were used. Mice were housed in a temperature- and humidity-controlled facility with a 12-h light/dark cycle at an ambient temperature of 19–22°C. All mice had free access to food and water throughout the study. Experiments were conducted during the light phase. Randomization was not performed to assign subjects. A total of 22 male mice were used in this study and number of animals per experiment described under figure legends (Figure 2 A - H), 5-HT uptake experiment for does dependent (N=4 mice for Vehicle and CHIR99021), time course effect (N=3 mice for Vehicle and CHIR99021), t-GSK3ß, p(S9)-GSK3ß levels (N=3 mice for Vehicle and CHIR99021), 5-HT kinetics (N=4 mice for Vehicle and CHIR99021), SERT surface biotinylation study (N=4 mice for Vehicle and CHIR99021) and SERT phosphorylation experiment (N=4 mice for Vehicle and CHIR99021). The study design is shown in Figure 1. Mice were subjected to rapid decapitation using small sharp animal guillotine without prior anesthesia between 9:00 a.m. and 12:00 p.m. to obtain the brain. Animals were kept away from the area of sacrifice before decapitation to minimize stress and handling. They proceeded as gently as possible to minimize the level of discomfort and pain to the animals.

Preparation of crude striatal synaptosomes

Mice were subjected to rapid decapitation, brains removed and striata, containing dorsal striatum (caudate putamen) and ventral striatum (nucleus accumbens) were dissected on ice. The striatal tissues were suspended immediately in cold 0.32 M sucrose in 5 mM HEPES, pH 7.4 (sucrose buffer), homogenized on ice and the homogenates were centrifuged at 1000 x g for 10 min at 4°C. The resultant supernatants were centrifuged at 12,000 x g for 20 min and the pellets containing the synaptosomes, myelin and mitochondria (Gray & Whittaker 1962) were resuspended in sucrose buffer. The protein concentration of each synaptosome preparation was determined by DC protein assay.

SERT functional assay (5-HT Uptake) in striatal synaptosomes

SERT function was assayed as described previously (Samuvel et al. 2005). As shown in figure legends, CHIR99021 or vehicle were incubated with striatal synaptosomes (30 – 50 µg) at 37°C in 0.5 ml of Krebs-Ringer buffer (KRH-assay buffer) (25 mM Na_2HCO_3, 124 mM NaCl, 5 mM KCl, 5 mM $MgSO_4$, 1.5 mM $CaCl_2$, 10 mM glucose, 0.1 mM pargyline and 0.1 mM ascorbic acid pH 7.3, saturated with 95% O_2, 5% CO_2). [^{3}H]5-HT uptake was measured using 50 nM of [^{3}H]5-HT (specific activity: 45.3 Ci/mmol), at 37°C for 4 min with or without SERT blocker 100 nM fluoxetine. SERT specific [^{3}H]5-HT uptake is obtained by subtracting [^{3}H]5-HT accumulation in the presence of fluoxetine from the total

[^{3}H]5-HT accumulation in the absence of fluoxetine. To do SERT kinetic analysis (K_m, V_{max}), [^{3}H]5-HT was mixed with unlabeled 5-HT and a range of 10 nM to 500 nM of 5-HT was used. At the end of assay, the synaptosomes were harvested by rapid filtration through 0.3% polyethylenimine coated GF-B filters using Brandel Cell Harvester (Brandel Inc., Gaithersburg, MD). and the filters were washed three times with 5 ml cold stop buffer (KRH buffer with 1 μM fluoxetine). The amount of radioactivity bound to filter was counted using a MicroBeta2 LumiJET liquid scintillation counter (Perkin Emler Inc., Waltham, MA). Non-Linear curve fits of uptake data used to generalize Michaelis-Menten equation to determine V_{max} and K_m values of SERT.

Surface biotinylation and immunoblotting in striatal synaptosomes

Determination of surface SERT levels in the synaptosomes using surface protein biotinylation was carried out as described previously (Samuvel et al. 2005, Annamalai et al. 2020). Synaptosomes (300 μg) were pretreated with CHIR99021 or vehicle at 37°C in KRH-assay buffer for the indicated time as given in figure legends. Synaptosomes were collected by centrifugation (12,000 x g for 20 min, 4°C) and subjected to biotinylation by incubating with EZ link NHS-Sulfo-SS-biotin (1 mg/1 mg protein) for 30 min at 4°C in ice-cold PBS/Ca/Mg buffer (138 mM NaCl, 2.7 mM KCl, 1.5 mM KH_2PO_4, 9.6 mM Na_2HPO_4, 1 mM $MgCl_2$, 0.1 mM $CaCl_2$, pH 7.3). At end of the biotinylation, the same buffer containing 100 mM glycine was used to quench excess NHS-Sulfo-SS-biotin. The biotinylated synaptosomes were then solubilized in radioimmunoprecipitation assay buffer (RIPA buffer) (10 mM Tris-HCl, pH 7.5, 150 mM NaCl, 1 mM EDTA, 1% Triton X-100, 0.1% SDS, and 1% sodium deoxycholate) supplemented with protease (1 μg/ml aprotinin, 1 μg/ml leupeptin, 1 μM pepstatin, and 250 μM phenylmethylsulfonyl fluoride) and phosphatase inhibitors (10 mM sodium fluoride, 50 mM sodium pyrophosphate, 5 mM sodium orthovanadate, and 1 μM okadaic acid) cocktails. The solubilizates were centrifuged at 25,000 x g for 30 min. Supernatants with equal amounts of proteins were incubated with 60 μl of NeutrAvidin agarose beads at 4°C for overnight to isolate biotinylated proteins. The extract with NeutrAvidin agarose beads were centrifuged at 25,000 g for 30 min and the supernatants (represents non-biotinylated intracellular proteins) were collected in fresh tubes. NeutrAvidin agarose beads were washed three times with RIPA buffer. Avidin bound proteins (represents biotinylated proteins residing on the membrane surface) were eluted with 45 μl of 2X Laemmli sample buffer and separated by 7.5 % SDS-PAGE along with total cell lysate (20 μl of total extract (750 μl), after incubation with NeutrAvidin agarose beads. The separated proteins were transferred on to polyvinylidene difluoride membrane (PVDF) overnight at 4°C and probed with SERT specific SR-12 antibody (1:2500 dilutions). The blots were visualized by using enhanced ECL reagents. The blots were stripped and reprobed with anti-calnexin antibody (1:5000 dilutions) to validate the loading protein levels as well to check for any contamination of biotinylated proteins with intracellular proteins. Calnexin is expressed in endoplasmic reticulum and used as an intracellular marker. The protein bands were quantified using NIH Image J software [version 1.48j] to ensure that results are within the linear range of the film exposure. The relative immunoreactivity of biotinylated representing the surface was normalized to total SERT immunoreactivity. The total SERT immunoreactivity was normalized with total calnexin.

SERT phosphorylation in striatal synaptosomes

5.0 mCi ^{32}P carrier-free orthophosphate (1 mg protein/1 ml) was added to striatal synaptosomes (350 μg) that were suspended in Krebs-bicarbonate buffer (25 mM Na_2HCO_3, 124 mM NaCl, 5 mM KCl, 1.5 mM $CaCl_2$, 5 mM $MgSO_4$, 10 mM glucose, pH 7.3, saturated with 95% O_2, 5% CO_2) and incubated at 37°C for 45 min on a continuously shaking platform. Following this step, different concentrations of CHIR99021 (in μM: 0.5, 1.0, 2.5, 5.0, 10.0) or vehicle was added and incubated further for another 15 min at 37°C. Synaptosomes were pelleted down by centrifugation and resuspended in RIPA buffer containing protease and phosphatase inhibitors (composition as given under “surface biotinylation and immunoblotting”). Synaptosomes were solubilized by passing through a 25-gauge needle 10 times and then by shaking for 1 hour at 4°C. Clear supernatants obtained following centrifugation of the samples at 25,000 x g for 40 min at 4°C were subjected to immunoprecipitation with SR-12 antibody (Sundaramurthy et al. 2017, Rajamanickam et al. 2015, Annamalai et al. 2012, Ramamoorthy et al. 2007, Jayanthi et al. 2005, Samuvel et al. 2005). The samples were then incubated with protein A sepharose beads (50 μl) to pull down immunoadsorbents. The immunoprecipitates adsorbed to protein A sepharose were washed with RIPA buffer and extracted with 50 μl Laemmli sample buffer by incubating for 30 min at 22°C and subjected to 10 % SDS-PAGE. The dried gels were exposed to radiographic films and ^{32}P radiolabeled SERT proteins were detected on autoradiograms. Autoradiograms from multiple exposures (1-3 days) were scanned and digitized to evaluate the ^{32}P-labeled SERT band densities (arbitrary units) within the linear range of film exposures of the same experiment using NIH ImageJ software [version 1.48j].

Site-directed mutagenesis

Serine (S) residues (S44 and S48) located in hSERT intracellular N-tail domains were mutated to alanine (A) residues using the Quickchange site-directed mutagenesis kit according to the manufacturer’s instructions. Mutations and absence of any unexpected mutations in full hSERT cDNA were confirmed twice by sequencing using sense and antisense primers.

Cell culture and transfections

Human embryonic kidney 293 cells (HEK-293) was obtained from ATCC (RRID: CVCL_0045) listed under Cellosaurus, and commonly misidentified cell line by the International Cell Line Authentication Committee (ICALC; https://iclac.org/databases/cross-contaminations/). HEK-293 were cultured in a mixture of DMEM supplemented with 10% (v/v) FBS, 100 units/ml penicillin (Gibco, Cat# 15140-122), 100μg/ml of streptomycin (Gibco, Cat# 15140-163) and 2 mM glutamine (Gibco, Cat# 25030-081) in a 5% CO_2 humidified atmosphere of 95% air and 5% CO_2. Cells maximum number of passages up to 15 were used in the study. We have not authenticated HEK-293 cells after purchase from ATCC and is not listed as misidentified cell line by the ICLAC (International Cell Line Authentication Committee). Trypsinized cells were seeded in 24 well plates (10 X 10^4/well) for uptake assays and (7.5 X 10^4/well) for siRNA interference studies or in 12 well plates (25 X 10^4/well) for biotinylation experiments. Transient transfections were carried using Lipofectamine™ 2000 according to manufacturer’s instructions and 0.3 μg/well or 0.6 μg/

well of cDNA (hSERT-WT or SERT mutants with GSK3β-S9A or empty vector pcDNA3 at a ratio of 1:1) for uptake or biotinylation assays. Experiments were performed 24 hours after transfection.

siRNA interference of GSK3αβ

The interference of GSK3α/ß was performed in HEK-293 cells with On-TARGETplus human GSK3α/ß siRNA-SMARTpool small interfering RNA (siRNA) specific to GSK3αß. The nonspecific scrambled sequence was used as a control. Cells were transfected with siRNA duplexes (100 nM) using Lipofectamine 2000 according to the manufacturer's instructions. After 16 h transfection with siRNA, cells were transfected with respective wild-type hSERT or hSERT-S48A (150 ng/well). After 24 h, [^{3}H]5-HT uptake assays and total and phospho-GSK3ß expression immunoblot analysis were performed as described below.

Detection of total and phospho-GSK3ß expression in striatal synaptosomes and transfected HEK-293 Cells

Striatal synaptosomes (50 μg) were treated with CHIR99021 (0.316, 0.625, 1.25, 2.5, 5.0, 10.0 μM) or vehicle and incubated for 15 min at 37°C. HEK-293 cells transfected with hSERT plus GSK3α/ß siRNA-SMARTpool or hSERT plus nonspecific scrambled sequence siRNA. Synaptosomes or transfected HEK-293 cells were extracted with RIPA buffer and transferred on to PVDF membrane as described above under "surface biotinylation and immunoblotting in striatal synaptosomes" and **"**cell surface protein biotinylation and detection of hSERT in transfected HEK-293 cells." The blots were probed with total GSK3ß or phosphor(S9)-GSKß antibodies (1:2000 dilutions) to determine the dose effect of CHIR99021 on total GSK3ß and phospho(S9)-GSK3ß levels in synaptosomes and the effect of GSK3α/ß siRNA-SMARTpool on the expression of total GSK3ß and phosphor(S9)-GSK3ß. The same blots after stripping were reprobed with calnexin antibody to evaluate any nonspecific effects of siRNA transfection in HEK-293 cells and loading controls as described previously (Rajamanickam et al. 2015).

Measurement of hSERT function in transfected HEK-293 Cells

[^{3}H]5-HT uptake was performed as described previously (Sundaramurthy et al. 2017, Rajamanickam et al. 2015, Ramamoorthy et al. 2007). The transfected HEK-293 cells were washed with prewarmed KRH assay buffer. Cells were treated with vehicle or CHIR99021 or kinase modulators (ß-PMA, Akt-X, KN-93, PD169316 or PP2) at 37°C as indicated in the Figure legends. The cells were incubated with 30 nM radiolabeled [^{3}H]5-HT (specific activity: 29 Ci/mmol) for 10 minutes at 37°C and the uptake was terminated by removing the radiolabel followed by washing the radiolabeled cells twice with stop buffer. For saturation analysis, labelled [^{3}H]5-HT was mixed with unlabeled 5-HT ranging from 50 nM to 4,000 nM. Nonspecific [^{3}H]5-HT uptake is defined as the accumulation in the presence of 100 nM fluoxetine and was subtracted from the total accumulated counts (CPM). Non-specific background was also compared using cells transfected with empty pcDNA3 vector alone. The cells were lysed with 400 μl of Optiphase Supermix scintillant and the radioactivity was measured using MicroBeta2 LumiJET liquid scintillation counter (Perkin Emler Inc., Waltham, MA). Three different passages of HEK-293 cells were used and uptake was

performed in duplicates or triplicates and results are presented as mean ± SD. V_{max} and K_m values for 5-HT uptake were determined by non-linear curve fits and the values were plotted 5-HT uptake against the concentration of 5-HT using Michaelis-Menten equation.

Cell surface protein biotinylation and detection of hSERT in transfected HEK-293 Cells

Transiently transfected HEK-293 cells were grown in 12 well plates, and treated with vehicle or CHIR99021 at 37°C as indicated in the figure legends. Cells were then subjected to biotinylation using cell membrane impermeable EZ link NHS-Sulfo-SS-biotin (0.5 mg/ml, 30 min at 4°C) in ice-cold PBS/Ca/Mg buffer as described previously (Rajamanickam et al. 2015, Sundaramurthy et al. 2017). Biotinylation was quenched by incubating the cells with 100 mM glycine in ice-cold PBS/Ca/Mg buffer for 15 min at 4°C. The cells were lysed with cold RIPA buffer supplemented with protease and phosphatase inhibitors at 4°C for an hour and by passing through a 26-gauge needle six times. Cell lysates were centrifuged at 25,000 g for 30 min and the supernatants were collected in fresh tubes. Equal amounts of proteins were incubated with 60 μl of NeutrAvidin agarose beads at 4°C for overnight. The extract with NeutrAvidin agarose beads were centrifuged at 25,000 g for 30 min and the supernatants (represents non-biotinylated intracellular proteins) were collected in fresh tubes. NeutrAvidin agarose beads were washed three washes with RIPA buffer. Avidin bound proteins (represents biotinylated proteins resides on membrane surface) were eluted with 45 μl of 2X Laemmli sample buffer and separated by 7.5 % SDS-PAGE along with total cell lysate, and lysates after incubation with NeutrAvidin agarose beads. Immunoblotting of SERT and calnexin proteins using specific antibodies as well as quantification and analysis of protein band densities were performed as described under “Surface Biotinylation and Immunoblotting in Striatal Synaptosomes.”. Because of observed variations in hSERT protein expression levels that are associated with transient transfections, cotransfections, and SERT mutations, it was necessary to adjust the time of film exposure to visualize bands. Therefore, direct quantitative comparisons of SERT immunoblots between experiments/figures are not possible. However, in each immunoblot, appropriate controls were included for parallel analyses.

Metabolic labeling and detection of GSK3β induced hSERT phosphorylation in transfected HEK-293 Cells

Cells were metabolically labeled with [^{32}P] orthophosphate as described previously (Ramamoorthy et al. 2007, Ramamoorthy et al. 1998). Briefly transiently transfected cells were incubated with 1 mCi/ml [^{32}P] orthophosphate for 1 h in phosphate-free DMEM media and solubilized with RIPA buffer containing protease and phosphatase inhibitors. hSERT protein was immunoprecipitated using SR-12 SERT-specific polyclonal antibody (2 μl/mg extract) and captured by protein A-Sepharose beads. The beads were washed three times with RIPA buffer and immunoprecipitated hSERT was eluted in 45 μl of 2X Laemmli buffer by incubating the beads for 30 mins at 22°C. The eluted proteins were separated by 10% SDS-PAGE. The gels were dried and exposed to HyBlot CL autoradiography films and ^{32}P radiolabeled hSERT was visualized by autoradiography. Multiple exposure (2-6 days) were evaluated by digital quantification using NIH image J software [version 1.48j] to ensure that the results are within the linear range of the film exposure.

Measurement of hSERT internalization from surface membrane (endocytosis) in transfected HEK-293 Cells

Reversible biotinylation was performed as described (Sundaramurthy et al. 2017, Rajamanickam et al. 2015, Samuvel et al. 2005). HEK 293 cells were transfected with hSERT or hSERT-S48A. Cells were cooled rapidly to 4 °C to inhibit endocytosis by washing with cold PBS/Ca-Mg buffer and surface biotinylated with membrane impermeable and disulfide-cleavable biotin (sulfo-NHS-SS-biotin). Free biotinylating reagent was removed by quenching with glycine. SERT endocytosis was initiated by incubating cells with prewarmed PBS/Ca-Mg buffer containing CHIR99021 (2.5 μM) or vehicle for 30 min at 37 °C. At the end of incubations, the reagents were removed, and fresh pre-chilled PBS/Ca-Mg buffer was added to stop the endocytosis. The cells were then washed and incubated twice with 250 μM sodium 2-mercaptoethanesulfonate (MesNa), a membrane impermeable reducing agent in PBS/Ca-Mg buffer for 20 min to dissociate the biotin from the cell surface-resident proteins via disulfide exchange. To define total surface biotinylated SERTs, one well of biotinylated cells was not subjected to reduction with MesNa, and directly processed for extraction followed by isolation by avidin beads. To define MesNa-accessible SERTs, another well of cells was treated with MesNa immediately following biotinylation at 4 °C to reveal the quantity of surface SERT biotinylation that MesNa can reverse efficiently. Following treatments, cells were solubilized in RIPA buffer. Separation of biotinylated hSERT from non-biotinylated proteins using NeutrAvidin beads, SDS-PAGE, immunoblotting of SERT and calnexin proteins, and quantification and analysis of protein band densities were performed as described under “cell surface protein biotinylation and detection of hSERT in transfected HEK-293 cells.” Internalized biotinylated SERT from surface membrane was calculated as: biotinylated SERT treated with vehicle or CHIR99021 at 37°C after MesNa stripped – MesNa resistant SERT band.

Measurement of hSERT insertion/delivery (exocytosis) to the plasma membrane in transfected HEK-293 Cells

Using biotinylating reagent, SERT insertion into the plasma membrane was measured as previously described (Samuvel et al. 2005). HEK 293 cells were transfected with hSERT-WT or hSERT-S48A. After washing cells with cold PBS/Ca-Mg buffer the cell membrane-impermeable sulfo-NHS-biotin (1 mg/ml) in PBS/Ca-Mg buffer containing CHIR99021(2.5 μM) or the vehicle (pre-warmed at 37 °C) was added to the cells and incubated further for the indicated time periods at 37 °C (trafficking permissive condition). In parallel, similar solutions, but prechilled to 4°C were added to other set of wells and incubated at 4°C (trafficking nonpermissive condition). Following incubations, cells were washed, and unused sulfo-NHS-biotin was quenched by incubating the cells with 100 mM glycine in ice-cold PBS/Ca/Mg buffer for 15 min. The cells then were solubilized in RIPA buffer and biotinylated SERT protein was separated from non-biotinylated proteins using NeutrAvidin beads. Biotinylated proteins were eluted from beads and resolved by SDS-PAGE. Biotinylated hSERT inserted into the plasma membrane (surface) were visualized with SERT-specific SR-12 antibody. Biotinylated transferrin receptor (TfR) and calnexin were analyzed by stripping and reprobing the blot with TfR and calnexin antibody to validate our approach. The accumulation of biotinylated hSERT, TfR and calnexin was measured and

quantified the band densities as described above under “cell surface protein biotinylation and detection of hSERT in transfected HEK-293 cells.”

Data and statistical analysis

Appropriate controls were included in each experiment. The statistical analyses were calculated by comparing respective controls that were performed in parallel in that particular experiment and reported in each figure. Blinding was not implemented in the experiments and the data analysis. Studies including mouse striatal synaptosomes and HEK-293 cells were exploratory and not pre-registered. No statistical method was used to determine the sample size calculation. The number of animals needed to detect differences between treatments and assays statistically was based on our published studies (Annamalai et al. 2020, Sundaramurthy et al. 2017, Rajamanickam et al. 2015, Annamalai et al. 2012, Ramamoorthy et al. 2007, Samuvel et al. 2005, Ramamoorthy et al. 1998). No exclusion or inclusion criteria were used. All values are expressed as mean ± standard deviation (SD). Figures were presented with bar graph showing all points. One-way or two-way analysis of variance was used, followed by *post hoc* testing (Bonferroni) for pair-wise comparisons. Student’s t-test was used to compare two data sets. A value of $P < 0.05$ was considered statistically significant. Specific statistical analyses, statistical data, significant and non-significant P-values and the number of samples used in each experiment are reported in each figure legend. Microsoft Excel (Mac-2019) and GraphPad Prism 8 (RRID:SCR_002798 GraphPad, San Diego, CA) were used for data analysis and statistical evaluations. GraphPad Prism 8 was used to generate figures. ImageJ 1.52a (National Institutes of Health, USA) was used for digital quantifications of bands from digitized films.

RESULTS

Pharmacological inhibition of GSK3α/ß upregulates SERT function in mouse striatal synaptosomes

GSK3 is constitutively active in a cell (Doble & Woodgett 2003). CHIR99021 is a highly selective GSK3α/ß inhibitor (Bennett et al. 2002). Therefore, we treated mouse striatal synaptosomes with CHIR99021 and examined whether GSK3α/ß activity regulates endogenous SERT-mediated 5-HT uptake. CHIR99021 pretreatment enhanced 5-HT uptake both in a concentration and time-dependent manners (Figure 2A and 2D respectively). Treatment with 0.316 μM, 0.625 μM, 1.25 μM, 2.5 μM, 5.0 μM and 10.0 μM of CHIR99021 for 15 min elevated 5-HT uptake with a maximum stimulation (175.7 ± 29.52% of vehicle) at 5 μM (Figure 2A). In parallel, we analyzed the levels of total GSK3ß and inhibitory phospho(S9)-GSK3ß following CHIR99021 treatment. GSK3ß inhibitors increase inhibitory phospho(S9)-GSK3ß level and studies used this as a measure to indicate the inhibition of GSK3ß activity (Chen et al. 2007, Monaco et al. 2018, Rajamanickam et al. 2015). Consistent with the dose-dependent effect of CHIR99021 on 5-HT uptake, CHIR99021 treatment concurrently increased inhibitory phospho(S9)-GSK3ß in a dose-dependent manner without altering the total GSK3ß (Figure 2B, 2C). At 10 μM, CHIR99021 gradually increased 5-HT uptake when pretreated for 5, 7.5, 15, 20, 30, and 60 mins (Figure 2D). We observed a significant effect of time, treatment of CHIR99021 as well as time and treatment interactions on elevated 5-HT uptake. CHIR99021 treatment showed a significant increase in

SERT-mediated 5-HT transport after 15 min pretreatment (177.8 ± 44.39% of the corresponding vehicle) reaching a maximum at 30 min (274.1 ± 25.10% of the corresponding vehicle), and no further increase was seen when the pretreatment was continued for up to 60 min (Figure 2D).

Blocking GSK3 activity enhances 5-HT transport kinetics and surface SERT expression in striatal synaptosomes

We determined the kinetics of 5-HT uptake (Michaelis-Menten constant, $K_{m,}$ and maximal velocity, V_{max}) after pharmacologically blocking GSK3α/ß activity in striatal synaptosomes. CHIR99021 treatment significantly increased the maximal velocity (V_{max}) and the apparent affinity of SERT for 5-HT (Figure 2E). Maximum velocity (V_{max}) was 4.610 ± 1.770 pmol/mg protein/min for vehicle treatment and 6.649 ± 2.691 pmol/mg protein/min for CHIR99021 treatment (P =0.0222, paired Student's t-test). 5-HT apparent affinity (K_m) was 106.2 ± 35.160 nM following vehicle treatment and 52.24 ± 38.750 nM after CHIR99021 treatment (P =0.0212, paired Student's t-test).

To assess if increased SERT V_{max} following GSK3α/ß inhibition is attributable to an increased presence of surface SERT, we performed cell membrane-impermeant protein biotinylation/immunoblot assay. Cell surface SERT levels were determined in striatal synaptosomes following treatment with vehicle or CHIR99021 (2.5 μM, 15 min). The results from surface biotinylation showed an increased surface density of SERT in CHIR99021-treated synaptosomes compared to vehicle-treated ones (Figure 2G). Quantitation of biotinylated surface SERT band densities showed a significant increase (76.15 ± 15.57%) in surface SERT levels following CHIR99021 treatment compared to vehicle treatment. It should be noted that the total level of SERT did not change with CHIR99021 treatment (Figure 2F). There was no difference in the density of calnexin (intracellular endoplasmic reticulum protein) in the total fractions when compared between vehicle and CHIR99021 (Figure 2F). An undetectable level of calnexin was present in the biotinylated fractions (Figure 2G) indicating that the surface-biotinylation procedure did not biotinylate intracellular SERT and other proteins.

Inhibition of GSK3ß reduces SERT phosphorylation in striatal synaptosomes

Several kinases regulate the activity of SERT via phosphorylation (Reviewed in Ramamoorthy et al. 2011, Bermingham & Blakely 2016). Therefore, next we examined if GSK3α/ß mediates its effect through phosphorylating SERT. Striatal synaptosomes were ^{32}P-metabolically labeled, treated with vehicle or different concentrations of CHIR99021, and autoradiography technique was performed to identify phosphorylated SERT. Consistent with our previous study (Rajamanickam et al. 2015, Samuvel et al. 2005), immunoprecipitates obtained with SERT-specific antibody revealed ^{32}P-labelled SERT bands (~94-98 kDa) (Figure 2H). Quantitated densities of ~94-98 kDa ^{32}P -SERT bands are shown as a bar graph. Compared to vehicle, treatment with 0.5 μM, 1.0 μM, 2.5 μM, 5.0 μM, and 10.0 μM of CHIR99021 for 15 min caused a dose-dependent decrease in SERT phosphorylation. Phosphorylation of ~94-98 kDa ^{32}P -SERT bands was significantly reduced at 2.5 μM CHIR99021 (61.58 ± 8.514% of vehicle), and a further reduction was also evident at higher concentrations (Figure 2H).

Pharmacological inhibition of GSK3α/ß upregulates hSERT in HEK-293 cells

The data in Figure 2 reveal that GSK3α/ß is involved in the regulation of endogenous SERT activity, apparent 5-HT affinity, surface expression, and phosphorylation in mouse striatal synaptosomes. To characterize further and understand the cellular mechanisms involved in the GSK3α/ß-mediated SERT regulation, we used a heterologous transient expression approach. Similar to mouse synaptosomes, CHIR99021 pretreatment of HEK-293 cells transfected with hSERT stimulated 5-HT uptake in a concentration and time-dependent manner (Figure 3A and 3B). Treatment with 0.316 μM, 0.625 μM, 1.25 μM, 2.5 μM and 5.0 μM of CHIR99021 for 45 min progressively enhanced 5-HT uptake. While an increase in 5-HT uptake at 0.625 μM is significant (% increase: 58.177 ± 18.765), significant maximum stimulation was observed at 1.25 and 2.5 μM (% increase: 81.781 ± 21.984, 82.581 ± 11.885 respectively), and no further increase was seen at 5.0 μM (Figure 3A). At 2.5 μM, CHIR99021 produced a time-dependent increase in 5-HT uptake following 5, 10, 15, 30, 45 min of treatment. A significant rise in 5-HT uptake was observed at 15 min (% increase: 84.12 ± 30.45) and reached a maximum at 30 min compared to vehicle (% increase: 114.703 ± 7.650) (Figure 3B). CHIR99021 treatment did not increase 5-HT uptake any further, and the maximum uptake was apparent up to 60 min. We observed significant effect of time and treatment. There was also significant time and treatment interaction. Following these dose and time course analyses, 2.5 μM of CHIR99021 and a treatment time of 45 min were used for further experiments. Our previous study demonstrated that this dose of CHIR99021 is shown to be effective in inhibiting GSK3ß (Rajamanickam et al. 2015). CHIR99021 up to 8 μM has been used in studies testing the role of GSK3 in cell models (Tu et al. 2017, Thorne et al. 2015, Ying et al. 2008, Langlands et al. 2018, Sineva & Pospelov 2010).

Blocking GSK3 activity enhances 5-HT transport kinetics and surface hSERT expression in HEK-293 cells

The kinetic analysis of 5-HT uptake (Michaelis-Menten constant, K_m, and maximal velocity, (V_{max}) in HEK-293 cells transfected with hSERT showed that CHIR99021 treatment resulted in a significant increase in the maximal velocity (V_{max}) (P=0.0096, t-test) and a nonsignificant increase in K_m (P=0.0716, t-test). Maximum velocity (V_{max}) was 22.68 ± 1.876 pmol/10^6cells/min for vehicle-treated cells and 40.95 ± 6.519 pmol/10^6cells/min for CHIR99021-treated cells. Apparent 5-HT affinity (K_m) for vehicle-treated cells was 423.6 ± 91.79 nM and CHIR99021-treated cells was 904.4 ± 329.4 nM (Figure 3C).

To assess if increased hSERT V_{max} following GSK3α/ß inhibition is attributable to increased surface hSERT as in striatal synaptosomes (Figure 2G), cell surface hSERT levels were determined in HEK-293 cells transfected with hSERT following treatment with vehicle or CHIR99021. The results from surface biotinylation studies showed increased cell surface density of hSERT in CHIR99021-treated cells compared to vehicle-treated cells (Figure 3E). Quantitation of band densities of surface hSERT protein showed a significant increase in cell surface hSERT levels following CHIR99021 treatment compared to vehicle treatment. The total level of hSERT did not change following CHIR99021 treatment (Figure 3D). The level of calnexin in the total fraction did not differ significantly between vehicle and CHIR99021 treatments (Figure 3D). Calnexin was undetectable in biotinylated fractions (Figure 3E).

GSK3-mediated regulation of SERT is dependent on serine residue at position 48 in hSERT

GSK3ß is known to regulate protein function by phosphorylating serine and threonine residues (Ali et al. 2001, Beurel et al. 2015). SERT is a phosphoprotein, and phosphorylation is known to affect SERT function and stability (Rajamanickam et al. 2015, Annamalai et al. 2012, Zhang et al. 2007, Ramamoorthy et al. 2007, Samuvel et al. 2005, Ramamoorthy & Blakely 1999, Ramamoorthy et al. 1998). The S44 and S48 sites in the SERT are consensus phosphorylation sites for GSK3. To gain further insight, we examined if the putative S44 and S48 sites in hSERT are involved in GSK3-mediated hSERT regulation. We substituted serine 44 and 48 in hSERT individually with alanine (hSERT-S44A, hSERT-S48A, respectively) to prevent phosphorylation. SERT mutants were expressed in HEK-293 cells and studied for the ability of CHIR99021 to stimulate their activity (Figure 4A). Compared to hSERT-WT, hSERT-S44A and hSERT-S48A displayed reduced 5-HT uptake (pmol/10^6cells/min, hSERT-WT: 0.5268 ± 0.0437, hSERT-S44A: 0.2809 ± 0.0195, hSERT-S48A: 0.2994 ± 0.0957). Exposure of HEK-293 cells expressing hSERT-WT, or hSERT-S44A to CHIR99021 stimulated 5-HT uptake compared to vehicle (Figure 4A). Remarkably, the CHIR99021-induced stimulation of 5-HT uptake was completely absent in the cells expressing hSERT-S48A mutant. There was a significant difference between hSERT-WT and hSERT-S48A following CHIR99021 treatment (Figure 4A).

Inhibition of GSK3α/ß by siRNA knockdown upregulates hSERT-WT but not hSERT-S48A in HEK-293 cells

To unequivocally confirm that GSK3α/β inhibition upregulates SERT, we knocked down GSK3α/β expression in HEK-293 cells using GSK3α/β-specific siRNA. Western blot analysis verified a significant reduction in both total and phospho(S9)-GSK3ß following GSK3α/β-specific siRNA transfection compared to that of scrambled-siRNA (Figure 4B). Total calnexin was similar in all siRNA-transfected cells (not shown). GSK3α/β-specific siRNA, but not the control scrambled siRNA, significantly enhanced hSERT activity corroborating the involvement of GSK3α/β in SERT regulation (Figure 4C). Next, we tested the role of S48A in GSK3-mediated SERT regulation. As shown in Figure 4C, there was no significant effect of GSK3α/β knockdown on hSERT-S48A activity. A significant difference was evident between hSERT-WT and hSERT-S48A following GSK3 knockdown by GSK3α/β siRNA (Figure 4C). Thus, these results confirm that the effect of GSK3α/β is specific for hSERT, and that hSERT-S48A mutant abrogates the GSK3α/β-mediated regulation.

Co-expression of wild-type and constitutively active GSK3β, but not an inactive form of GSK3β, inhibits 5-HT uptake in HEK-293 cells

A potential mechanism by which GSK3 regulates hSERT is likely by altering SERT phosphorylation. Since Ser48 is required for CHIR99021-induced stimulation of SERT, we next sought to determine whether Ser48 is phosphorylated in hSERT following GSK3 modulations. We tested if stimulation of GSK3ß activity inhibits hSERT activity and increases hSERT phosphorylation by co-expressing a constitutively active GSK3ß-S9A construct with hSERT in HEK-293 cells. Figure 4D shows the expression of endogenous GSK3ß in HEK-293 cells, and the transfected HA-tagged WT-GSK3ß, constitutively active

GSK3β (GSKβ-S9A), and an inactive GSK3ß (GSK3ß-K85A) (higher size due to HA-tagging). Active GSK3β-S9A and inactive GSK3ß-K85A have been used by others to study the role of GSK3ß in several model systems (Stambolic & Woodgett 1994, McManus et al. 2005). Consistent with our notion, Figure 4D illustrates 5-HT uptake in cells expressing hSERT plus HA-tagged WT-GSK3β or active HA-GSK3β-S9A was significantly lower compared to 5-HT uptake in cells co-transfected with empty vector pcDNA3 or inactive HA-GSK3β-K85A. CHIR99021 treatment of cells transfected with hSERT-WT plus vector control pcDNA3 resulted in increased SERT activity (Figure 4D). However, CHIR99021 treatment of cells co-expressing hSERT-WT and active GSK3β-S9A or WT-GSK3β resulted in complete prevention/reversal of SERT inhibition (Figure 4D). We next sought to determine the effect of active GSK3β-S9A co-expression on non-phosphorylatable hSERT mutants. Compared to pcDNA3, co-transfection of active GSK3β-S9A with wild-type, S44A, hSERT but not with hSERT-S48A significantly reduced 5-HT uptake (Figure 4E). Cotransfection with active GSK3β-S9A revealed a significant difference between hSERT-WT and hSERT-S48A.

GSK3ß-mediated hSERT phosphorylation is absent in hSERT-S48A

The results obtained from using hSERT mutants (Figure 4A and 4E) demonstrate that the serine 48 of hSERT is involved in GSK3ß-mediated SERT regulation; however, it does not inform whether the GSK3ß mediates its effect through modulating hSERT phosphorylation, and more so, specifically at S48 residue. Therefore, we examined hSERT phosphorylation using ^{32}P-metabolically labeled HEK-293 cells expressing hSERT-WT or hSERT-S48A with or without co-expressing active GSK3β-S9A. Consistent with our previous study (Rajamanickam et al. 2015, Samuvel et al. 2005), immunoprecipitates obtained from using a SERT-specific antibody revealed ^{32}P-labelled hSERT bands (~94-98 kDa) (Figure 4F). Quantitated densities of ^{32}P-hSERT bands are shown in a bar graph. Compared to pcDNA3, GSK3β-S9A co-transfection with hSERT-WT significantly enhanced ^{32}P-labelling of hSERT bands (Figure 4F, lanes 1 and 2). However, there was no significant difference in the ^{32}P-labelling of hSERT between cells co-transfected with hSERT-S48A plus pcDNA3 and cells co-transfected with hSERT-S48A plus GSK3β-S9A (Figure 4F lanes 3 and 4). Thus, the results confirm a significant difference in the GSK3β-mediated phosphorylation of hSERT between hSERT-WT and hSERT-S48A mutant (Figure 4F, lanes 2 and 4). Due to low level of hSERT phosphorylation observed in cells co-transfected with hSERT-WT plus pcDNA3 and also in cells co-transfected with hSERT-S48A plus pcDNA3 (Figure 4F lanes 1 and 3), it is difficult to determine whether S48A mutation impacts the level of hSERT basal phosphorylation.

Akt, CaMKII, PKC, p38 MAPK, and Src are not involved in GSK3ß-mediated SERT regulation via hSERT-S48.

Notably, protein kinases and phosphatases that regulate SERT function (Reviewed Ramamoorthy et al. 2011, Bermingham & Blakely 2016) including PKC (Moore et al. 2013), p38 MAPK (Thornton et al. 2008), Src (Goc et al. 2014) and protein phosphatase 2A (Sutherland et al. 1993, Zhang et al. 2003) also modulate GSK3 phosphorylation, dephosphorylation, and activity. Therefore, we examined if S48 in the hSERT is involved in Akt, CaMKII, PKC, p38 MAPK, and Src -mediated SERT regulation. Consistent with

published studies, treatment with inhibitors for Akt (Rajamanickam et al. 2015), CaMKII (Annamalai et al. 2012), p38 MAPK (Samuvel et al. 2005), and Src (Annamalai et al. 2012) (Akt-X, KN-93, PD169316, PP2 respectively), or with PKC activator (ß-PMA) produced a significant reduction in 5-HT uptake in cells expressing the hSERT-WT or hSERT-S48A (Figure 5A). These results indicate that Akt, CaMKII, p38 MAPK, Src and PKC are not involved in the GSK3ß-mediated SERT basal expression through S48 phosphorylation.

GSK3ß-mediated alteration in SERT kinetics is attenuated with hSERT-S48A

Next, we determined the effects of constitutively active GSK3β-S9A and S48-phosphorylation of hSERT on 5-HT transport kinetics by co-expressing active GSK3β-S9A with hSERT-WT or hSERT-S48A. Two-way RM ANOVA analysis revealed a significant effect of GSK3ß-S9A co-expression, S48A mutation in hSERT, and interactions of GSK3ß-S9A co-expression (Figure 5B). Co-expression of active GSK3β-S9A with hSERT-WT induced a significant decrease in the maximal velocity of 5-HT transport (12.410 ± 0.308 pmol/10^6cells/min) compared to control pcDNA3 co-transfection (22.420 ± 2.488 pmol/10^6cells/min). However, co-expressing GSK3β-S9A with hSERT-S48A did not alter the V_{max}. (Figure 5B). The V_{max} in hSERT-S48A + pcDNA3 transfected cells is 8.368 ± 0.187 pmol/10^6cells/min, as well as hSERT-S48A + GSK3β-S9A transfected cells is 9.918 ± 1.735 pmol/10^6cells/min (Figure 5B). hSERT-S48A showed reduced V_{max}. Co-expression of active GSK3β-S9A with hSERT-WT or hSERT-S48A did not alter SERT apparent substrate affinity significantly. The K_m values in nM: 1476 ± 280.00 for hSERT-S48A + pcDNA3, 891.5 ± 498.50 for hSERT-S48A + GSK3β-S9A compared to 1141 ± 379.80 for hSERT-WT + pcDNA3, 1101 ± 107.20 for hSERT-WT + GSK3β-S9A respectively.

GSK3ß activity fails to increase hSERT-S48A surface expression in HEK-293 cells

Inhibition of GSK3α/ß using CHIR99021 resulted in enhanced hSERT activity (Figure 3A and 3B) with a concomitant increase in the surface hSERT (Figure 3E). Mutating S48 into a non-phosphorylatable Ala in hSERT prevented CHIR99021-mediated increase of SERT activity (Figure 4A). Therefore, we investigated the impact of S48A mutation on basal and GSK3ß-mediated regulation of surface hSERT. Total expression of both hSERT-WT and hSERT-S48A were comparable with or without co-expression of active GSK3β-S9A (Figure 5C). However, hSERT-S48A surface expression was significantly reduced with concomitant increase in intracellular pool compared to hSERT-WT (Figure 5D and 5E) consistent with reduced V_{max} observed in hSERT-S48A (Figure 5B). Consistent with the effect on the V_{max} of hSERT-WT, co-expression of active GSK3β-S9A significantly decreased surface hSERT-WT with a concomitant increase in intracellular levels; however, that effect of GSK3β-S9A was not seen with hSERT-S48A (Figure 5D and 5E).

Blocking GSK3ß activity fails to promote hSERT-S48A internalization and insertion into the plasma membrane

Increased surface hSERT could result from either reduced internalization or enhanced insertion of SERT or a net result of both. We examined the internalization of hSERT-WT and hSERT-S48A in HEK-293 cells under basal/constitutive conditions, and following treatment with CHIR99021. We used a reversible biotinylation strategy and quantitated the fraction of biotinylated surface hSERT that moved into an intracellular compartment as described

previously (Rajamanickam et al. 2015). Briefly, a non- permeant sodium 2-mercaptoethanesulfonate (MesNa) was used to remove the biotin moiety from the biotinylated proteins that were remaining on the surface at the end of the vehicle or CHIR99021 treatment. Therefore, the biotinylated SERT resistant (inaccessible) to MesNa treatment is accountable as internalized SERT from the surface plasma membrane. Thus, incubating the cells at the optimal trafficking temperature of 37 °C in the absence or presence of CHIR99021 before and after MesNa reversal of surface biotinylation allows evaluating SERT internalization. Consistent with our observations presented in Figure 5C, the total biotinylated hSERT-S48A was lesser than wild-type hSERT (Figure 6A, lanes 1 and 2). MesNa treatment after biotinylation (30 min at 4°C) (Figure 6A, lanes 3 and 4). revealed an undetectable level of total biotinylated hSERT-WT and hSERT-S48A indicating the successful removal of biotin from the biotinylated surface SERT, and very little internalization at 4°C. Following vehicle treatment at 37°C for 30 min, internalized-biotinylated hSERT-WT was seen (Figure 6A, lane 5). This increase represents constitutive internalization (e.g., basal endocytosis). A significant difference was seen between hSERT-WT (Figure 6A, lanes 5 and 6) and hSERT-S48A (Figure 6A, lanes 7 and 8) internalization following CHIR99021 treatment (Figure 6B). CHIR99021 treatment for 30 min at 37°C significantly decreased constitutive wild-type SERT endocytosis when compared with vehicle treatment. In contrast to hSERT-WT, CHIR99021 treatment did not change hSERT-S48A internalization (Figure 6B). The absence of biotinylated intracellular calnexin was indicative of the integrity of the cell membrane and the observed biotinylated SERT derived from the surface plasma membrane (Figure 6A).

Next, we examined if CHIR99021 treatment alters SERT delivery to the plasma membrane. HEK-293 cells were transfected with hSERT-WT + pcDNA3, or hSERT-S48A + pcDNA3. Delivery of hSERT to the cell surface was determined by performing biotinylation at trafficking-permissive temperature, 37°C, and compared with biotinylation at trafficking-non-permissive temperature, 4°C as described previously (Samuvel et al. 2005). The presence of an excessive amount of the membrane-impermeant biotinylation agent during the incubation period should label the hSERT proteins that are inserted/delivered to the plasma membrane with biotin. Figure 6C and 6D shows the results of biotinylation experiments in which plasma membrane insertion of hSERT was measured following vehicle or CHIR99021 treatment. Incubation at 37°C showed increased hSERT membrane insertion (lanes 5, 6, 7 and 8) when compared to incubation at 4°C (lanes 1, 2, 3 and 4) (Figure 6C). A significant difference was observed between hSERT-WT and hSERT-S48A membrane insertion following CHIR99021 treatment (Figure 6D). CHIR99021 treatment at 37°C for 30 min increased hSERT-WT membrane insertion significantly. However, we observed that CHIR99021 treatment with hSERT-S48A did not produce a significant difference in hSERT-S48A insertion when compared to vehicle treatment. There was no difference in the level of biotinylated calnexin between 37°C and 4°C incubation and vehicle *versus* CHIR99021-treated cells indicating that changes in biotinylated hSERT proteins at 37°C represents newly delivered hSERT to the surface plasma membrane. As to validate our experimental approach, we also determined the level of biotinylated transferrin receptor (TfR) as an additional marker of recycling. A higher level of biotinylated TfR (insertion) was observed at 37°C in comparison with 4°C. CHIR99021 treatment did not affect the level

of biotinylated TfR (Figure 6C), indicating that CHIR99021 treatment did not interfere with the normal recycling of proteins in HEK-293 cells.

DISCUSSION

GSK3α/ß is a serine/threonine-protein kinase that modulates several protein substrates in the brain (Doble & Woodgett 2003, Beaulieu et al. 2009, Beaulieu et al. 2007, Woodgett 1990). It has been shown that GSK3ß in the hippocampus and striatum is involved in the regulation of anxiety and other social behaviors including depression-like behavior (Latapy et al. 2012, Pardo et al. 2016). Targeting GSK3ß selectively in 5-HT neurons impacts neuronal firing, 5-HT release and 5-HT-related behavior (Zhou et al. 2012). A meta-analysis of postmortem brain samples from depressed patients showed reduced SERT levels in important limbic areas including striatum (Kambeitz & Howes 2015). These findings indicate that GSK3ß, which is constitutively active in a cell (Doble & Woodgett 2003), plays a critical role in serotonergic system, including the regulation of SERT. Our study provides direct evidence to this notion by demonstrating that GSK3α/ß inhibition by CHIR99021 stimulates SERT activity, Vmax, surface expression, increases the apparent affinity for 5-HT and decreases SERT phosphorylation in neuronal striatal synaptosomes. In addition, decreased SERT phosphorylation was evident with concomitant increase in inhibitory phospho(S9)-GSK3ß. These findings suggest that GSK3α/ß activity supports 5-HT transport in striatal 5-HT terminals by sustaining basal SERT surface expression via phosphorylation and perhaps by modulating or stabilizing the conformation of surface-resident SERTs to access 5-HT to its binding site or other 5-HT dependent effects on conformational movements of the transporter related to transport cycle. Studies have shown that activation or inhibition of receptors, kinases, and phosphatases alter apparent substrate (5-HT) affinity (K_m) (Ansah et al. 2003, Zhu et al. 2006, Chang et al. 2012, Zhu et al. 2005, Samuvel et al. 2005, Jayanthi et al. 2005) and intrinsic SERT activity (Ramamoorthy et al. 2007). Our previous study demonstrated that inhibition of p38 MAPK altered both SERT V_{max} and K_m in midbrain synaptosomes (Samuvel et al. 2005).

Amino acid sequence analysis showed two (S44, S48) potential GSK3α/ß consensus phosphorylation sites S(44)NGYS(48)AVPS(53) (underlined) in the hSERT N-tail suggesting a possibility that GSK3α/ß regulates SERT function through phosphorylation (Ramamoorthy et al. 1993). Mutational analysis of these putative sites and studying in a heterologous expression cell model provides direct evidence for GSK3α/ß-mediated SERT phosphorylation. Here we show that acute pharmacological inhibition of GSK3α/ß by CHIR99021 or expression of total and phospho-form of GSK3ß stimulates hSERT-mediated 5-HT uptake in HEK-293 cells, thus establishing a role of GSK3ß in SERT functional regulation. GSK3ß-inhibitory effect of CHIR99021 is also associated with a significant increase in the maximal velocity of 5-HT transport. The observed increase in cell-surface hSERT without any change in the level of total hSERT following CHIR99021 treatment suggests that GSK3α/ß activity regulates hSERT function by regulating hSERT cellular compartmentalization and not via synthesis or degradation. The increase in surface hSERT following CHIR99021 treatment indeed results from reduced transporter internalization and increased membrane insertion. The doses of CHIR99021 that produce elevated SERT activity are higher than IC_{50} reported for CHIR99021 to inhibit GSKα (10 nM) or GSK3ß

(6.7 nM) (Ring et al. 2003). Several studies have used higher doses of CHIR99021, up to 8 μM, to determine the role of GSK3 (Tu et al. 2017, Thorne et al. 2015, Ying et al. 2008, Langlands et al. 2018, Sineva & Pospelov 2010, Rajamanickam et al. 2015). At present, we cannot exclude the possibility that CHIR99021 affects other kinases or targets at higher doses.

Replacement of predicted GSK3α/ß-target phosphorylation site Ser48 but not Ser44 with non-phosphorylatable Ala prevented the stimulatory effect of CHIR99021 treatment. Furthermore, CHIR99021 treatment decreased the internalization and increased the plasma membrane insertion of hSERT-WT, but failed to modulate hSERT-S48A internalization or plasma membrane insertion. These results establish the pivotal role of Ser48 in GSK3α/ß-mediated basal hSERT regulation. This is further supported by the fact that the stimulatory effect of GSK3α/ß knockdown is diminished on the hSERT-S48A mutant. Expression of recombinant GSKß-S9A further supports the involvement of Ser48 in GSK3ß-mediated hSERT regulation. Remarkably, the inhibition of hSERT activity by active GSK3ß-S9A was absent when co-expressed with hSERT-S48A mutant but not with hSERT-S44A. We directly examined the ability of GSK3ß to modulate phosphorylation of hSERT-WT and hSERT-S48A. Indeed, the active GSK3ß-S9A stimulated basal phosphorylation of hSERT-WT but not that of hSERT-S48A. Also, while active GSK3ß-S9A co-expression decreased the V_{max}, surface expression, it failed to have an impact on those of the hSERT-S48A mutant. Surprisingly, hSERT-S48A mutant was sensitive to Akt, CaMKII, p38 MAPK, Src-kinase inhibition and PKC activation similar to hSERT-WT. Collectively, these results suggest that S48 is the target site that is essential for GSK3ß mediated constitutive hSERT regulation, but not for Akt, CaMKII, p38 MAPK, Src kinase or PKC mediated hSERT regulation. However, further studies are needed to determine whether GSK3 phosphorylates SERT directly, and also to determine the identity of pre-synaptic receptor linked upstream signals modulating the GSK3 activity.

Previous studies exploring protein kinases-mediated regulation of SERT function found that changes in SERT-maximal velocity correlated with levels of transporter surface expression except for a few (Reviewed in and see references therein: Ramamoorthy et al. 2011, Bermingham & Blakely 2016). Regulated internalization, plasma membrane delivery, and stability of hSERT contribute to surface expression and 5-HT transport (Qian et al. 1997, Steiner et al. 2008, Sundaramurthy et al. 2017, Rajamanickam et al. 2015, Samuvel et al. 2005, Jayanthi et al. 2005, Ramamoorthy & Blakely 1999, Rahbek-Clemmensen et al. 2014). We showed that while PKC activation triggers hSERT internalization, inhibition of p38 MAPK and Akt decreases plasma membrane insertion (Rajamanickam et al. 2015, Samuvel et al. 2005, Jayanthi et al. 2005). Studies also document that p38 MAPK, Src, and PKG regulate SERT activity by a trafficking-independent mechanism (Steiner et al. 2009, Annamalai et al. 2012, Ramamoorthy et al. 2007, Zhu et al. 2005). We reported that Akt regulates hSERT plasma membrane delivery by regulating trafficking pathways at the level of late endosomes, lysosomes, and other intracellular organelles (Rajamanickam et al. 2015). Here, our characterization of the hSERT-S48A mutant reveals that while total expression of hSERT-S48A is similar to that of hSERT-WT, hSERT-S48A has decreased surface expression and increased intracellular levels suggesting a role for Ser48 phosphorylation in

maintaining the basal internalization, plasma membrane insertion and/or recycling rate of hSERT.

Previously we identified Thr276, Tyr42, Tyr 142, Tyr350 and Tyr358 as phosphorylation sites involved in PKG- and Src- mediated SERT regulation (Annamalai et al. 2012, Ramamoorthy et al. 2007). This study reveals Ser48 as a phosphorylation site in hSERT, and the phosphorylation of this site mediated by active GSK3ß supports basal SERT activity and surface expression. Given the fact that GSK3α/ß inhibition increases basal SERT function and surface expression, removal of Ser48 phosphorylation as in hSERT-S48A mutant should have enhanced SERT activity and surface expression. On the contrary, the hSERT-S48A mutant showed less surface expression despite having intact total SERT protein. Currently, this paradoxical phenomenon is not clear. To better understand this conundrum, future studies should focus on establishing detailed trafficking pathways (both basal and regulated) involving Ser48 phosphorylation of hSERT.

GSK3 recognizes serine or threonine that are four residues N-terminal to a template-phosphorylated serine or threonine (S/T-X-X-X-S/T(P) (Ubersax & Ferrell 2007, Doble & Woodgett 2003). The consensus S48 site for GSK3α/ß phosphorylation in SERT is S(48)AVPS (53). It is possible that S53 serves as a template-phosphorylated residue allowing GSK3 to prime phosphorylate S48 site. We are currently investigating the identity of a kinase that template-phosphorylates S53 to prepare S48 as a phosphorylation site for active GSK3ß.

While this study provides evidence that GSK3α/ß supports endogenous basal SERT phosphorylation, activity, and surface expression in mouse brain striatum, our conclusion for the requirement of SERT-Ser48 phosphorylation in GSK3-mediated SERT regulation is derived from the results obtained with a heterologous SERT expression model using HEK-293 cells. While the effects of GSK3α/ß inhibition on SERT V_{max} and surface SERT are comparable between striatal synaptosomes expressing native SERTs and HEK-293 cells heterologously expressing hSERT, there are differences between the two models. (i) 5-HT K_m values are lower in the striatum and higher in HEK-293 cells. (ii) While CHIR99021 treatment decreased 5-HT K_m values in the striatum, a nonsignificant increase in 5-HT K_m values is observed in HEK-293 cells. It is possible that the observed difference is due to a lack of other endogenous factors that may be critical for GSK3α/ß activity to modulate SERT affinity to its substrate 5-HT. In this juncture, further studies are required to determine the contribution of GSK3α/ß on basal SERT expression in different brain regions. In summary, there are some limitations in interpreting the data from the HEK-293 cell model because of the heterologous nature of the SERT expression. It is imperative that Ser48 phosphorylation is further characterized in a native system.

In addition to the synthesis and degradation of 5-HT, 5-HT release and re-uptake are critical for normal 5-HT neurotransmission (Bengel et al. 1998). While SERT regulates extracellular 5-HT to activate 5-HT receptors, auto-receptor 5-HT_{1B} decreases 5-HT release as a feedback mechanism (Sari 2004, Riad et al. 2000). 5-HT_{1B} receptors interact with GSK3ß and facilitate 5-HT_{1B}-mediated regulation of 5-HT release (Chen et al. 2011). Findings from the current study provide new evidence that GSK3ß modulates 5-HT clearance via regulating

SERT phosphorylation, apparent 5-HT affinity and trafficking. Additional evidence suggests that the activation or inhibition of 5-HT_{1B} receptors regulate SERT function (Daws et al. 2000, Hagan et al. 2012), while 5-HT_{1B} receptor-kinase signaling engaged in SERT regulation remains unknown. Though speculative, GSK3ß may be involved in 5-HT_{1B} receptor-mediated SERT regulation since GSK3ß regulates HT_{1B} receptor signaling cascades (Zhou et al. 2012, Chen et al. 2011, Chen et al. 2009). Thus, a possible model is that GSK3ß might function as a hub or a signal integrator for 5-HT release and clearance (Polter & Li 2011). Because of the specific involvement of GSK3ß in 5-HT_{1B} auto-receptor regulated 5-HT release in the axon terminals of 5-HT neurons (Chen et al. 2009, Chen et al. 2011, Zhou et al. 2012), we focused on studying GSK3ß. Nonetheless, our findings do not rule out the involvement of GSK3α in the regulation of SERT and needs further investigation.

Interestingly, pharmacological inhibition of GSK3 and specific deletion of GSK3ß in 5-HT neurons elicit antidepressant-like effect (Zhou et al. 2012, Chen et al. 2011, Li & Jope 2010). SERT blockers are known as antidepressants (Holmes et al. 2002, Mayorga et al. 2001), and studies have shown that SERT inhibitors regulate GSK3ß phosphorylation (Okamoto et al. 2010). GSK3 inhibitor lithium has been used in the treatment of bipolar disorder (O'Brien & Klein 2009, Jope 2011). Dysregulated GSK3 activity and SERT expression have been implicated in the pathophysiology of bipolar disorder (Li et al. 2010, Muneer 2017, Cannon et al. 2006, Gijsman et al. 2004, Tolmunen et al. 2004, Beaulieu et al. 2009, Shah et al. 2009). Merging with our findings that GSK3 supports SERT functional expression, it is reasonable to speculate that SERT-regulatory motifs represent new therapeutic targets for bipolar disorder, and useful biomarkers for lithium therapy.

Dysregulated SERT and 5-HT neurotransmission are evident in mood disorders (Lesch et al. 1996, Murphy et al. 2013, Moya et al. 2013, Hartley et al. 2012, Hahn & Blakely 2007, Murphy & Moya 2011, Cook et al. 1997, Murphy et al. 2004). A polymorphism of GSK3ß promotor and an increase in GSK-3 activity have been implicated in depression, suicide, mood, and other neurological disorders (Beurel et al. 2015, Karege et al. 2007, Karege et al. 2012, Serretti et al. 2008, Benedetti et al. 2004). Also, of interest is an interaction between the promoter variants of GSK3ß and hSERT, which has been shown to influence clinical antidepressant response to sleep deprivation (Benedetti et al. 2012). Thus, abnormal regulation of GSK3-mediated SERT may exist in neuropsychiatric disorders. Notably, autism associated hSERT coding mutant Ala56 exhibits enhanced 5-HT uptake, basal phosphorylation, 5-HT affinity, and altered interaction with SERT-interacting proteins (Quinlan et al. 2020, Veenstra-VanderWeele et al. 2012, Prasad et al. 2009, Quinlan et al. 2019). Given that GSK3 modulates apparent affinity of SERT for 5-HT, and the close proximity of Ala56 to Ser48, possibilities exist that these two sites may interact to modulate SERT function. Thus, it would be interesting to examine whether perturbed characteristics of hSERT coding variant Ala56 are linked to GSK3 mediated hSERT-S48 phosphorylation.

In summary, our findings reveal that there may be an essential link between signaling pathways that regulate 5-HT release and clearance through GSK3ß in 5-HT terminals, and coordinated orchestrations of these cellular events are necessary for normal serotonergic neurotransmission and behavior.

Supplementary Material

Refer to Web version on PubMed Central for supplementary material.

ACKNOWLEDGMENTS

The work was supported by National Institute of Mental Health grant MH112731 (S.R.). We greatly acknowledge technical assistance from Santhanalakshmi Sundaramurthy who initiated earlier studies on GSK3-involvement in SERT regulation.

Abbreviations used:

5-HT	5-hydorxytryptamine (serotonin)
A	alanine
Akt	protein kinase B
ANOVA	analysis of variance
CaMKII	calmodulin-dependent protein kinase II
GSK3α/ß	glycogen synthase kinase-3α/ß
HEK-293	human embryonic kidney-293 cells
MesNa	2-mercaptoethanesulfonate
p38 MAPK	p38 mitogen-activated protein kinase
PKA	protein kinase A
PKC	protein kinase C
PKG	protein kinase G
RRID	Research resource identifier
S	serine
SDS-PAGE	sodium dodecyl sulfate-polyacrylamide gel electrophoresis
SERT	serotonin transporter
siRNA	small interfering RNA
SSRIs	selective serotonin reuptake inhibitors
Tyr	tyrosine
WT	wild-type

REFERENCES

Ali A, Hoeflich KP and Woodgett JR (2001) Glycogen synthase kinase-3: properties, functions, and regulation. Chem Rev, 101, 2527–2540. [PubMed: 11749387]

Annamalai B, Mannangatti P, Arapulisamy O, Shippenberg TS, Jayanthi LD and Ramamoorthy S (2012) Tyrosine phosphorylation of the human serotonin transporter: a role in the transporter stability and function. Mol Pharmacol, 81, 73–85. [PubMed: 21992875]

Annamalai B, Ragu Varman D, Horton RE, Daws LC, Jayanthi LD and Ramamoorthy S (2020) Histamine Receptors Regulate the Activity, Surface Expression, and Phosphorylation of Serotonin Transporters. ACS Chem Neurosci, 11, 466–476. [PubMed: 31916747]

Ansah TA, Ramamoorthy S, Montanez S, Daws LC and Blakely RD (2003) Calcium-dependent inhibition of synaptosomal serotonin transport by the alpha 2-adrenoceptor agonist 5-bromo-N-[4,5-dihydro-1H-imidazol-2-yl]-6-quinoxalinamine (UK14304). J Pharmacol Exp Ther, 305, 956–965. [PubMed: 12626658]

Ballenger JC (1999) Current treatments of the anxiety disorders in adults. Biol Psychiatry, 46, 1579–1594. [PubMed: 10599485]

Beaulieu JM, Gainetdinov RR and Caron MG (2007) The Akt-GSK-3 signaling cascade in the actions of dopamine. Trends Pharmacol Sci, 28, 166–172. [PubMed: 17349698]

Beaulieu JM, Gainetdinov RR and Caron MG (2009) Akt/GSK3 signaling in the action of psychotropic drugs. Annu Rev Pharmacol Toxicol, 49, 327–347. [PubMed: 18928402]

Benedetti F, Dallaspezia S, Lorenzi C, Pirovano A, Radaelli D, Locatelli C, Poletti S, Colombo C and Smeraldi E (2012) Gene-gene interaction of glycogen synthase kinase 3-beta and serotonin transporter on human antidepressant response to sleep deprivation. J Affect Disord, 136, 514–519. [PubMed: 22119086]

Benedetti F, Serretti A, Colombo C, Lorenzi C, Tubazio V and Smeraldi E (2004) A glycogen synthase kinase 3-beta promoter gene single nucleotide polymorphism is associated with age at onset and response to total sleep deprivation in bipolar depression. Neurosci Lett, 368, 123–126. [PubMed: 15351432]

Bengel D, Murphy DL, Andrews AM, Wichems CH, Feltner D, Heils A, Mossner R, Westphal H and Lesch KP (1998) Altered brain serotonin homeostasis and locomotor insensitivity to 3,4-methylenedioxymetamphetamine ("ecstasy") in serotonin transporter-deficient mice. Molecular Pharmacology, 53, 649–655. [PubMed: 9547354]

Bennett CN, Ross SE, Longo KA, Bajnok L, Hemati N, Johnson KW, Harrison SD and MacDougald OA (2002) Regulation of Wnt signaling during adipogenesis. J Biol Chem, 277, 30998–31004. [PubMed: 12055200]

Berger M, Gray JA and Roth BL (2009) The expanded biology of serotonin. Annu Rev Med, 60, 355–366. [PubMed: 19630576]

Bermingham DP and Blakely RD (2016) Kinase-dependent Regulation of Monoamine Neurotransmitter Transporters. Pharmacol Rev, 68, 888–953. [PubMed: 27591044]

Beurel E, Grieco SF and Jope RS (2015) Glycogen synthase kinase-3 (GSK3): regulation, actions, and diseases. Pharmacol Ther, 148, 114–131. [PubMed: 25435019]

Cannon DM, Ichise M, Fromm SJ et al. (2006) Serotonin transporter binding in bipolar disorder assessed using [11C]DASB and positron emission tomography. Biol Psychiatry, 60, 207–217. [PubMed: 16875929]

Carneiro AM, Airey DC, Thompson B, Zhu CB, Lu L, Chesler EJ, Erikson KM and Blakely RD (2009) Functional coding variation in recombinant inbred mouse lines reveals multiple serotonin transporter-associated phenotypes. Proc Natl Acad Sci U S A, 106, 2047–2052. [PubMed: 19179283]

Chang JC, Tomlinson ID, Warnement MR, Ustione A, Carneiro AM, Piston DW, Blakely RD and Rosenthal SJ (2012) Single molecule analysis of serotonin transporter regulation using antagonist-conjugated quantum dots reveals restricted, p38 MAPK-dependent mobilization underlying uptake activation. J Neurosci, 32, 8919–8929. [PubMed: 22745492]

Chen L, Salinas GD and Li X (2009) Regulation of serotonin 1B receptor by glycogen synthase kinase-3. Mol Pharmacol, 76, 1150–1161. [PubMed: 19741007]

Chen L, Zhou W, Chen PC, Gaisina I, Yang S and Li X (2011) Glycogen synthase kinase-3beta is a functional modulator of serotonin-1B receptors. Mol Pharmacol, 79, 974–986. [PubMed: 21372171]

Chen P, Gu Z, Liu W and Yan Z (2007) Glycogen synthase kinase 3 regulates N-methyl-D-aspartate receptor channel trafficking and function in cortical neurons. Mol Pharmacol, 72, 40–51. [PubMed: 17400762]

Cook EH Jr., Courchesne R, Lord C, Cox NJ, Yan S, Lincoln A, Haas R, Courchesne E and Leventhal BL (1997) Evidence of linkage between the serotonin transporter and autistic disorder. Molecular Psychiatry, 2, 247–250. [PubMed: 9152989]

Daws LC, Gould GG, Teicher SD, Gerhardt GA and Frazer A (2000) 5-HT(1B) receptor-mediated regulation of serotonin clearance in rat hippocampus in vivo. J Neurochem, 75, 2113–2122. [PubMed: 11032901]

Doble BW and Woodgett JR (2003) GSK-3: tricks of the trade for a multi-tasking kinase. J Cell Sci, 116, 1175–1186. [PubMed: 12615961]

Fozzard J (1989) Peripheral actions of 5-hydroxytryptamine. Oxford University Press, New York.

Frame S and Cohen P (2001) GSK3 takes centre stage more than 20 years after its discovery. Biochem J, 359, 1–16. [PubMed: 11563964]

Gijsman HJ, Geddes JR, Rendell JM, Nolen WA and Goodwin GM (2004) Antidepressants for bipolar depression: a systematic review of randomized, controlled trials. Am J Psychiatry, 161, 1537–1547. [PubMed: 15337640]

Goc A, Al-Husein B, Katsanevas K, Steinbach A, Lou U, Sabbineni H, DeRemer DL and Somanath PR (2014) Targeting Src-mediated Tyr216 phosphorylation and activation of GSK-3 in prostate cancer cells inhibit prostate cancer progression in vitro and in vivo. Oncotarget, 5, 775–787. [PubMed: 24519956]

Gray EG and Whittaker VP (1962) The isolation of nerve endings from brain: an electron-microscopic study of cell fragments derived by homogenization and centrifugation. J Anat, 96, 79–88. [PubMed: 13901297]

Grimes CA and Jope RS (2001) The multifaceted roles of glycogen synthase kinase 3beta in cellular signaling. Prog Neurobiol, 65, 391–426. [PubMed: 11527574]

Hagan CE, McDevitt RA, Liu Y, Furay AR and Neumaier JF (2012) 5-HT(1B) autoreceptor regulation of serotonin transporter activity in synaptosomes. Synapse, 66, 1024–1034. [PubMed: 22961814]

Hahn MK and Blakely RD (2007) The functional impact of SLC6 transporter genetic variation. Annu Rev Pharmacol Toxicol, 47, 401–441. [PubMed: 17067279]

Hartley CA, McKenna MC, Salman R, Holmes A, Casey BJ, Phelps EA and Glatt CE (2012) Serotonin transporter polyadenylation polymorphism modulates the retention of fear extinction memory. Proc Natl Acad Sci U S A, 109, 5493–5498. [PubMed: 22431634]

Holmes A, Yang RJ, Murphy DL and Crawley JN (2002) Evaluation of antidepressant-related behavioral responses in mice lacking the serotonin transporter. Neuropsychopharmacology, 27, 914–923. [PubMed: 12464448]

Jacobs B and Azmitia EC (1992) Structure and function of the brain serotonin system. Physiological Reviews, 72, 165–229. [PubMed: 1731370]

Jayanthi LD, Ramamoorthy S, Mahesh VB, Leibach FH and Ganapathy V (1994) Calmodulin-dependent regulation of the catalytic function of the human serotonin transporter in placental choriocarcinoma cells. J Biol Chem, 269, 14424–14429. [PubMed: 8182048]

Jayanthi LD, Samuvel DJ, Blakely RD and Ramamoorthy S (2005) Evidence for biphasic effects of protein kinase C on serotonin transporter function, endocytosis, and phosphorylation. Mol Pharmacol, 67, 2077–2087. [PubMed: 15774771]

Jope RS (2011) Glycogen synthase kinase-3 in the etiology and treatment of mood disorders. Front Mol Neurosci, 4, 16. [PubMed: 21886606]

Kambeitz JP and Howes OD (2015) The serotonin transporter in depression: Meta-analysis of in vivo and post mortem findings and implications for understanding and treating depression. J Affect Disord, 186, 358–366. [PubMed: 26281039]

Karege F, Perroud N, Burkhardt S, Fernandez R, Ballmann E, La Harpe R and Malafosse A (2012) Protein levels of beta-catenin and activation state of glycogen synthase kinase-3beta in major depression. A study with postmortem prefrontal cortex. J Affect Disord, 136, 185–188. [PubMed: 22036797]

Karege F, Perroud N, Burkhardt S, Schwald M, Ballmann E, La Harpe R and Malafosse A (2007) Alteration in kinase activity but not in protein levels of protein kinase B and glycogen synthase kinase-3beta in ventral prefrontal cortex of depressed suicide victims. Biol Psychiatry, 61, 240–245. [PubMed: 16876135]

Kent JM, Coplan JD and Gorman JM (1998) Clinical utility of the selective serotonin reuptake inhibitors in the spectrum of anxiety. Biol Psychiatry, 44, 812–824. [PubMed: 9807637]

Kugaya A, Seneca NM, Snyder PJ, Williams SA, Malison RT, Baldwin RM, Seibyl JP and Innis RB (2003) Changes in human in vivo serotonin and dopamine transporter availabilities during chronic antidepressant administration. Neuropsychopharmacology, 28, 413–420. [PubMed: 12589396]

Langlands AJ, Carroll TD, Chen Y and Nathke I (2018) Chir99021 and Valproic acid reduce the proliferative advantage of Apc mutant cells. Cell Death Dis, 9, 255. [PubMed: 29449562]

Latapy C, Rioux V, Guitton MJ and Beaulieu JM (2012) Selective deletion of forebrain glycogen synthase kinase 3beta reveals a central role in serotonin-sensitive anxiety and social behaviour. Philos Trans R Soc Lond B Biol Sci, 367, 2460–2474. [PubMed: 22826345]

Lesch K-P, Bengel D, Heils A et al. (1996) Association of anxiety-related traits with a polymorphism in the serotonin transporter gene regulatory region. Science, 274, 1527–1531. [PubMed: 8929413]

Li X and Jope RS (2010) Is glycogen synthase kinase-3 a central modulator in mood regulation? Neuropsychopharmacology, 35, 2143–2154. [PubMed: 20668436]

Li X, Liu M, Cai Z, Wang G and Li X (2010) Regulation of glycogen synthase kinase-3 during bipolar mania treatment. Bipolar Disord, 12, 741–752. [PubMed: 21040291]

Mayorga AJ, Dalvi A, Page ME, Zimov-Levinson S, Hen R and Lucki I (2001) Antidepressant-like behavioral effects in 5-hydroxytryptamine(1A) and 5- hydroxytryptamine(1B) receptor mutant mice. J Pharmacol Exp Ther, 298, 1101–1107. [PubMed: 11504807]

McManus EJ, Sakamoto K, Armit LJ, Ronaldson L, Shpiro N, Marquez R and Alessi DR (2005) Role that phosphorylation of GSK3 plays in insulin and Wnt signalling defined by knockin analysis. EMBO J, 24, 1571–1583. [PubMed: 15791206]

Miller KJ and Hoffman BJ (1994) Adenosine A3 receptors regulate serotonin transport via nitric oxide and cGMP. J Biol Chem, 269, 27351–27356. [PubMed: 7525554]

Monaco SA, Ferguson BR and Gao WJ (2018) Lithium Inhibits GSK3beta and Augments GluN2A Receptor Expression in the Prefrontal Cortex. Front Cell Neurosci, 12, 16. [PubMed: 29449801]

Moore SF, van den Bosch MT, Hunter RW, Sakamoto K, Poole AW and Hers I (2013) Dual regulation of glycogen synthase kinase 3 (GSK3)alpha/beta by protein kinase C (PKC)alpha and Akt promotes thrombin-mediated integrin alphaIIbbeta3 activation and granule secretion in platelets. J Biol Chem, 288, 3918–3928. [PubMed: 23239877]

Moya PR, Wendland JR, Rubenstein LM et al. (2013) Common and rare alleles of the serotonin transporter gene, SLC6A4, associated with Tourette's disorder. Mov Disord, 28, 1263–1270. [PubMed: 23630162]

Muneer A (2017) Wnt and GSK3 Signaling Pathways in Bipolar Disorder: Clinical and Therapeutic Implications. Clin Psychopharmacol Neurosci, 15, 100–114. [PubMed: 28449557]

Murphy DL, Lerner A, Rudnick G and Lesch KP (2004) Serotonin transporter: gene, genetic disorders, and pharmacogenetics. Mol Interv, 4, 109–123. [PubMed: 15087484]

Murphy DL and Moya PR (2011) Human serotonin transporter gene (SLC6A4) variants: their contributions to understanding pharmacogenomic and other functional GxG and GxE differences in health and disease. Curr Opin Pharmacol, 11, 3–10. [PubMed: 21439906]

Murphy SE, Norbury R, Godlewska BR, Cowen PJ, Mannie ZM, Harmer CJ and Munafo MR (2013) The effect of the serotonin transporter polymorphism (5-HTTLPR) on amygdala function: a meta-analysis. Mol Psychiatry, 18, 512–520. [PubMed: 22488255]

Nackenoff AG, Moussa-Tooks AB, McMeekin AM, Veenstra-VanderWeele J and Blakely RD (2016) Essential Contributions of Serotonin Transporter Inhibition to the Acute and Chronic Actions of Fluoxetine and Citalopram in the SERT Met172 Mouse. Neuropsychopharmacology, 41, 1733–1741. [PubMed: 26514584]

Norrholm SD, Horton DB and Dwoskin LP (2007) The promiscuity of the dopamine transporter: implications for the kinetic analysis of [3H]serotonin uptake in rat hippocampal and striatal synaptosomes. Neuropharmacology, 53, 982–989. [PubMed: 18022203]

O'Brien WT and Klein PS (2009) Validating GSK3 as an in vivo target of lithium action. Biochem Soc Trans, 37, 1133–1138. [PubMed: 19754466]

Okamoto H, Voleti B, Banasr M, Sarhan M, Duric V, Girgenti MJ, Dileone RJ, Newton SS and Duman RS (2010) Wnt2 expression and signaling is increased by different classes of antidepressant treatments. Biol Psychiatry, 68, 521–527. [PubMed: 20570247]

Owens MJ and Nemeroff CB (1994) Role of serotonin in the pathophysiology of depression: focus on the serotonin transporter. Clinical Chemistry, 40, 288–295. [PubMed: 7508830]

Pardo M, Abrial E, Jope RS and Beurel E (2016) GSK3beta isoform-selective regulation of depression, memory and hippocampal cell proliferation. Genes Brain Behav, 15, 348–355. [PubMed: 26749572]

Polter AM and Li X (2011) Glycogen Synthase Kinase-3 is an Intermediate Modulator of Serotonin Neurotransmission. Front Mol Neurosci, 4, 31. [PubMed: 22028682]

Prasad HC, Steiner JA, Sutcliffe JS and Blakely RD (2009) Enhanced activity of human serotonin transporter variants associated with autism. Philos Trans R Soc Lond B Biol Sci, 364, 163–173. [PubMed: 18957375]

Prasad HC, Zhu CB, McCauley JL, Samuvel DJ, Ramamoorthy S, Shelton RC, Hewlett WA, Sutcliffe JS and Blakely RD (2005) Human serotonin transporter variants display altered sensitivity to protein kinase G and p38 mitogen-activated protein kinase. Proc Natl Acad Sci U S A, 102, 11545–11550. [PubMed: 16055563]

Qian Y, Galli A, Ramamoorthy S, Risso S, DeFelice LJ and Blakely RD (1997) Protein kinase C activation regulates human serotonin transporters in HEK-293 cells via altered cell surface expression. J Neurosci, 17, 45–57. [PubMed: 8987735]

Quinlan MA, Krout D, Katamish RM, Robson MJ, Nettesheim C, Gresch PJ, Mash DC, Henry LK and Blakely RD (2019) Human Serotonin Transporter Coding Variation Establishes Conformational Bias with Functional Consequences. ACS Chem Neurosci, 10, 3249–3260. [PubMed: 30668912]

Quinlan MA, Robson MJ, Ye R, Rose KL, Schey KL and Blakely RD (2020) Ex vivo Quantitative Proteomic Analysis of Serotonin Transporter Interactome: Network Impact of the SERT Ala56 Coding Variant. Front Mol Neurosci, 13, 89. [PubMed: 32581705]

Rahbek-Clemmensen T, Bay T, Eriksen J, Gether U and Jorgensen TN (2014) The serotonin transporter undergoes constitutive internalization and is primarily sorted to late endosomes and lysosomal degradation. J Biol Chem, 289, 23004–23019. [PubMed: 24973209]

Rajamanickam J, Annamalai B, Rahbek-Clemmensen T, Sundaramurthy S, Gether U, Jayanthi LD and Ramamoorthy S (2015) Akt-mediated regulation of antidepressant-sensitive serotonin transporter function, cell-surface expression and phosphorylation. Biochem J, 468, 177–190. [PubMed: 25761794]

Ramamoorthy S, Bauman AL, Moore KR, Han H, Yang-Feng T, Chang AS, Ganapathy V and Blakely RD (1993) Antidepressant- and cocaine-sensitive human serotonin transporter: molecular cloning, expression, and chromosomal localization. Proc Natl Acad Sci U S A, 90, 2542–2546. [PubMed: 7681602]

Ramamoorthy S and Blakely RD (1999) Phosphorylation and sequestration of serotonin transporters differentially modulated by psychostimulants. Science, 285, 763–766. [PubMed: 10427004]

Ramamoorthy S, Giovanetti E, Qian Y and Blakely RD (1998) Phosphorylation and regulation of antidepressant-sensitive serotonin transporters. J Biol Chem, 273, 2458–2466. [PubMed: 9442097]

Ramamoorthy S, Samuvel DJ, Buck ER, Rudnick G and Jayanthi LD (2007) Phosphorylation of threonine residue 276 is required for acute regulation of serotonin transporter by cyclic GMP. J Biol Chem, 282, 11639–11647. [PubMed: 17310063]

Ramamoorthy S, Shippenberg TS and Jayanthi LD (2011) Regulation of monoamine transporters: Role of transporter phosphorylation. Pharmacol Ther, 129, 220–238. [PubMed: 20951731]

Riad M, Garcia S, Watkins KC, Jodoin N, Doucet E, Langlois X, el Mestikawy S, Hamon M and Descarries L (2000) Somatodendritic localization of 5-HT1A and preterminal axonal localization of 5-HT1B serotonin receptors in adult rat brain. J Comp Neurol, 417, 181–194. [PubMed: 10660896]

Ring DB, Johnson KW, Henriksen EJ et al. (2003) Selective glycogen synthase kinase 3 inhibitors potentiate insulin activation of glucose transport and utilization in vitro and in vivo. Diabetes, 52, 588–595. [PubMed: 12606497]

Samuvel DJ, Jayanthi LD, Bhat NR and Ramamoorthy S (2005) A role for p38 mitogen-activated protein kinase in the regulation of the serotonin transporter: evidence for distinct cellular mechanisms involved in transporter surface expression. J Neurosci, 25, 29–41. [PubMed: 15634764]

Sari Y (2004) Serotonin1B receptors: from protein to physiological function and behavior. Neurosci Biobehav Rev, 28, 565–582. [PubMed: 15527863]

Schindler AG, Messinger DI, Smith JS et al. (2012) Stress produces aversion and potentiates cocaine reward by releasing endogenous dynorphins in the ventral striatum to locally stimulate serotonin reuptake. J Neurosci, 32, 17582–17596. [PubMed: 23223282]

Seimandi M, Seyer P, Park CS, Vandermoere F, Chanrion B, Bockaert J, Mansuy IM and Marin P (2013) Calcineurin interacts with the serotonin transporter C-terminus to modulate its plasma membrane expression and serotonin uptake. J Neurosci, 33, 16189–16199. [PubMed: 24107951]

Serretti A, Benedetti F, Mandelli L, Calati R, Caneva B, Lorenzi C, Fontana V, Colombo C and Smeraldi E (2008) Association between GSK-3beta −50T/C polymorphism and personality and psychotic symptoms in mood disorders. Psychiatry Res, 158, 132–140. [PubMed: 17976739]

Shah MP, Wang F, Kalmar JH et al. (2009) Role of variation in the serotonin transporter protein gene (SLC6A4) in trait disturbances in the ventral anterior cingulate in bipolar disorder. Neuropsychopharmacology, 34, 1301–1310. [PubMed: 19037205]

Sineva GS and Pospelov VA (2010) Inhibition of GSK3beta enhances both adhesive and signalling activities of beta-catenin in mouse embryonic stem cells. Biol Cell, 102, 549–560. [PubMed: 20626347]

Stambolic V and Woodgett JR (1994) Mitogen inactivation of glycogen synthase kinase-3 beta in intact cells via serine 9 phosphorylation. Biochem J, 303 (Pt 3), 701–704. [PubMed: 7980435]

Steiner JA, Carneiro AM and Blakely RD (2008) Going with the flow: trafficking-dependent and -independent regulation of serotonin transport. Traffic, 9, 1393–1402. [PubMed: 18445122]

Steiner JA, Carneiro AM, Wright J et al. (2009) cGMP-dependent protein kinase Ialpha associates with the antidepressant-sensitive serotonin transporter and dictates rapid modulation of serotonin uptake. Mol Brain, 2, 26. [PubMed: 19656393]

Steinkellner T, Montgomery TR, Hofmaier T et al. (2015) Amphetamine action at the cocaine- and antidepressant-sensitive serotonin transporter is modulated by alphaCaMKII. J Neurosci, 35, 8258–8271. [PubMed: 26019340]

Sundaramurthy S, Annamalai B, Samuvel DJ, Shippenberg TS, Jayanthi LD and Ramamoorthy S (2017) Modulation of serotonin transporter function by kappa-opioid receptor ligands. Neuropharmacology, 113, 281–292. [PubMed: 27743931]

Sutherland C, Leighton IA and Cohen P (1993) Inactivation of glycogen synthase kinase-3 beta by phosphorylation: new kinase connections in insulin and growth-factor signalling. Biochem J, 296 (Pt 1), 15–19. [PubMed: 8250835]

Thorne CA, Wichaidit C, Coster AD, Posner BA, Wu LF and Altschuler SJ (2015) GSK-3 modulates cellular responses to a broad spectrum of kinase inhibitors. Nat Chem Biol, 11, 58–63. [PubMed: 25402767]

Thornton TM, Pedraza-Alva G, Deng B et al. (2008) Phosphorylation by p38 MAPK as an alternative pathway for GSK3beta inactivation. Science, 320, 667–670. [PubMed: 18451303]

Tolmunen T, Joensuu M, Saarinen PI, Mussalo H, Ahola P, Vanninen R, Kuikka J, Tiihonen J and Lehtonen J (2004) Elevated midbrain serotonin transporter availability in mixed mania: a case report. BMC Psychiatry, 4, 27. [PubMed: 15363105]

Tu C, Xu R, Koleti M and Zoldan J (2017) Glycogen synthase kinase-3 inhibition sensitizes human induced pluripotent stem cells to thiol-containing antioxidants induced apoptosis. Stem Cell Res, 23, 182–187. [PubMed: 28772167]

Ubersax JA and Ferrell JE Jr. (2007) Mechanisms of specificity in protein phosphorylation. Nat Rev Mol Cell Biol, 8, 530–541. [PubMed: 17585314]

Veenstra-VanderWeele J, Muller CL, Iwamoto H et al. (2012) Autism gene variant causes hyperserotonemia, serotonin receptor hypersensitivity, social impairment and repetitive behavior. Proc Natl Acad Sci U S A, 109, 5469–5474. [PubMed: 22431635]

Woodgett JR (1990) Molecular cloning and expression of glycogen synthase kinase-3/factor A. EMBO J, 9, 2431–2438. [PubMed: 2164470]

Ying QL, Wray J, Nichols J, Batlle-Morera L, Doble B, Woodgett J, Cohen P and Smith A (2008) The ground state of embryonic stem cell self-renewal. Nature, 453, 519–523. [PubMed: 18497825]

Zhang F, Phiel CJ, Spece L, Gurvich N and Klein PS (2003) Inhibitory phosphorylation of glycogen synthase kinase-3 (GSK-3) in response to lithium. Evidence for autoregulation of GSK-3. J Biol Chem, 278, 33067–33077. [PubMed: 12796505]

Zhang YW, Gesmonde J, Ramamoorthy S and Rudnick G (2007) Serotonin transporter phosphorylation by cGMP-dependent protein kinase is altered by a mutation associated with obsessive compulsive disorder. J Neurosci, 27, 10878–10886. [PubMed: 17913921]

Zhou W, Chen L, Paul J et al. (2012) The effects of glycogen synthase kinase-3beta in serotonin neurons. PLoS One, 7, e43262. [PubMed: 22912839]

Zhu CB, Blakely RD and Hewlett WA (2006) The proinflammatory cytokines interleukin-1beta and tumor necrosis factor-alpha activate serotonin transporters. Neuropsychopharmacology, 31, 2121–2131. [PubMed: 16452991]

Zhu CB, Carneiro AM, Dostmann WR, Hewlett WA and Blakely RD (2005) p38 MAPK activation elevates serotonin transport activity via a trafficking-independent, protein phosphatase 2A-dependent process. J Biol Chem, 280, 15649–15658. [PubMed: 15728187]

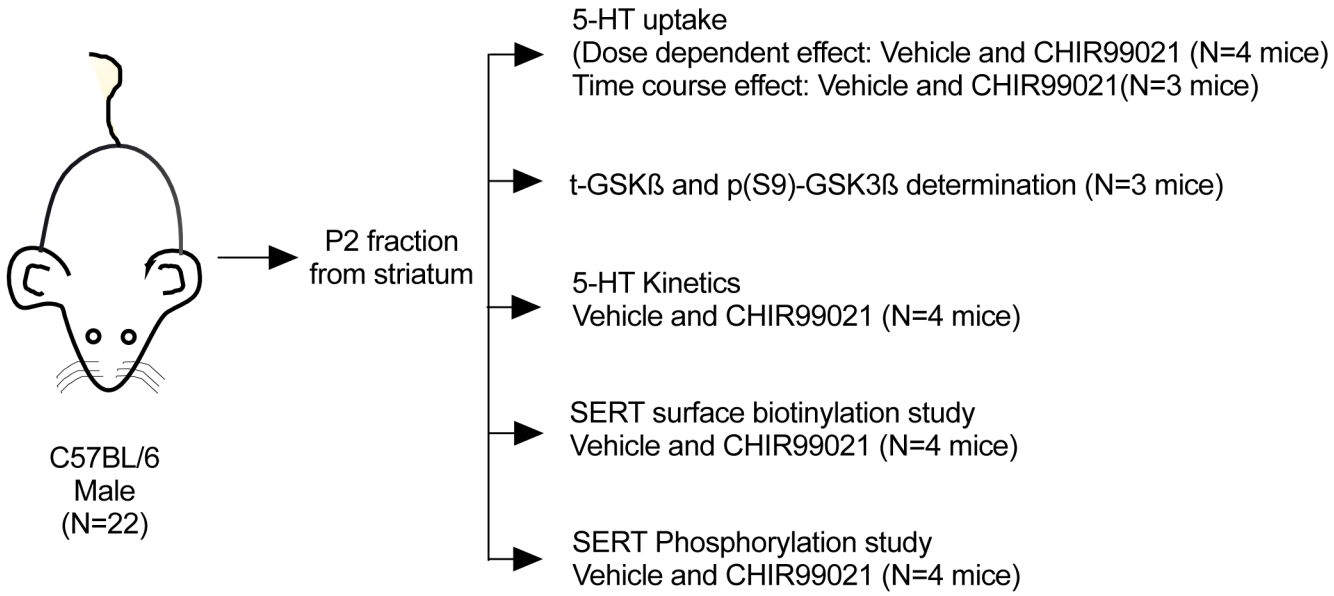

FIGURE 1. Animal numbers and experiments.
Refer “Materials and Methods” for more details.

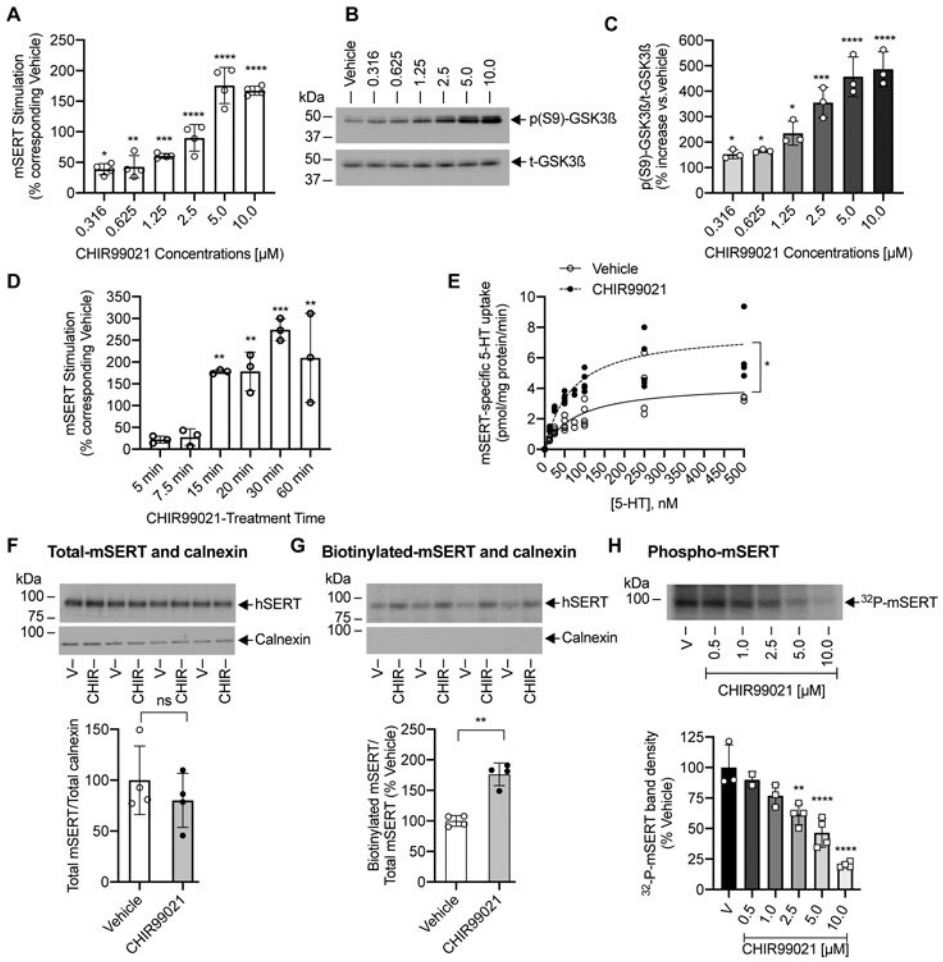

FIGURE 2. Effect of GSKα/ß inhibitor CHIR99021 on 5-HT uptake, t-GSK3ß and p(S9)-GSK3ß levels, SERT kinetics, SERT surface expression, and SERT phosphorylation in mouse striatal synaptosomes.

(A, B, C, D). 5-HT uptake and t-GSK3ß and p(S9)-GSK3ß levels. Mouse striatal synaptosomes were preincubated with vehicle or indicated concentrations of CHIR99021 for 15 min at 37°C **(A, B, C)** or preincubated with vehicle or 10 μM CHIR99021 for various times indicated **(D)**. [^{3}H]5-HT uptake assays, t-GSK3ß and p(S9)-GSK3ß immunoblots were conducted following the treatments. [^{3}H]5-HT uptake assays were performed in triplicates from one independent mouse, and each data point indicates the average of triplicates. **(A).** CHIR99021 pretreatment stimulates SERT activity in a dose-dependent manner (one-way ANOVA: $F_{(6,21)} = 64.21$, $P < 0.0001$). Bonferroni's multiple comparison test: *P =0.0202, **P =0.0089, ***P <0.0002, ****P <0.0001 compared with vehicle-treated control (N=4 mice, mean ± SD). **(B, C).** Dose dependent effect of CHIR99021 on t-GSK3ß and p(S9)-GSK3ß levels. A representative immunoblot of three independent experiments (3 mice) shows t-GSK3ß and p(S9)-GSK3ß (**B**) and Quantified p(S9)-GSK3ß normalized to t-GSK3ß (**C**). CHIR99021 pretreatment increased p(S9)-GSK3ß in a dose-dependent manner (one-way ANOVA: $F_{(6,14)} = 29.25$, $P < 0.0001$). Bonferroni's multiple comparison test: *P =0.0295, ***P =0.0001, ****P <0.0001 compared with vehicle (N=3 mice, mean ± SD). **(D).** CHIR99021 stimulates SERT activity in a time-dependent manner

(two-way ANOVA: time $F_{(5,10)}$ = 12.13, P =0.0006), CHIR99021 treatment $F_{(1,2)}$ = 37.92, P =0.0254), and time and CHIR99021 treatment interactions ($F_{(5,10)}$ = 11.16, P =0.0008). Bonferroni's multiple comparison test: **P =0.002 (15 min), **P =0.0019 (20 min), ***P <0.0005 (30 min), **P =0.0023 (60 min) compared with corresponding vehicle (N=3 mice, mean ± SD). **(E).** Effect of CHIR99021 on SERT kinetics. Striatal synaptosomes were treated with vehicle or CHIR99021 (2.5 μM) for 15 min at 37°C. SERT specific [^{3}H]5-HT uptake was measured using various concentrations of 5-HT. Assays were performed in triplicates from one independent mouse, and each data point indicates the average of triplicates. Non-Linear curve fits of uptake data for vehicle (N=4 mice) and CHIR99021 (N=4 mice) were shown (mean ± SD). *P =0.0222 (paired t-test) compared with vehicle. **(F** and **G).** Effect of CHIR99021 on surface SERT. Mouse striatal synaptosomes were preincubated with vehicle or CHIR99021 (2.5 μM) for 15 min at 37°C and cell surface biotinylation was performed. Striatal synaptosomes obtained from four independent mice, and all samples were run on the same gel. Immunoblots show total **(F)** and biotinylated SERT **(G)**. The presence of intracellular marker protein calnexin is shown under each SERT immunoblot. Quantified total SERT normalized to total calnexin and quantified biotinylated SERT normalized to total SERT were shown under the respective immunoblots. The SERT band densities in CHIR99021treated samples (N=4 mice) are shown relative to vehicle-treated samples (N=4 mice) (mean ± SD). **P =0.0023 significant difference and ns: non-significant effect compared with vehicle (Paired Student's t-test). **(H)**. Effect of CHIR99021 on SERT phosphorylation. Metabolically-[^{32}P]labeled striatal synaptosomes were treated with vehicle or indicated concentrations of CHIR99021 for 15 min at 37°C. Immunoprecipitated ^{32}P-labelled SERT was subjected to SDS-PAGE and autoradiography. A representative autoradiogram of four independent experiments (4 mice) shows ^{32}P-labelled SERT bands (~94-98 kDa). The band densities of ^{32}P-labelled SERT in CHIR99021treated samples (N=4 mice) are shown relative to vehicle-treated samples (N=4 mice) (mean ± SD). Each point represents data from one independent mouse. Due to very close values, some data points are merged. CHIR99021 treatment significantly decreased mSERT phosphorylation in a dose-dependent manner (one-way ANOVA: $F_{(5,14)}$ = 26.12, P <0.0001). Bonferroni's multiple comparison test: **P =0.0015, ****P <0.0001 compared with vehicle V: Vehicle, CHIR: CHIR99021.

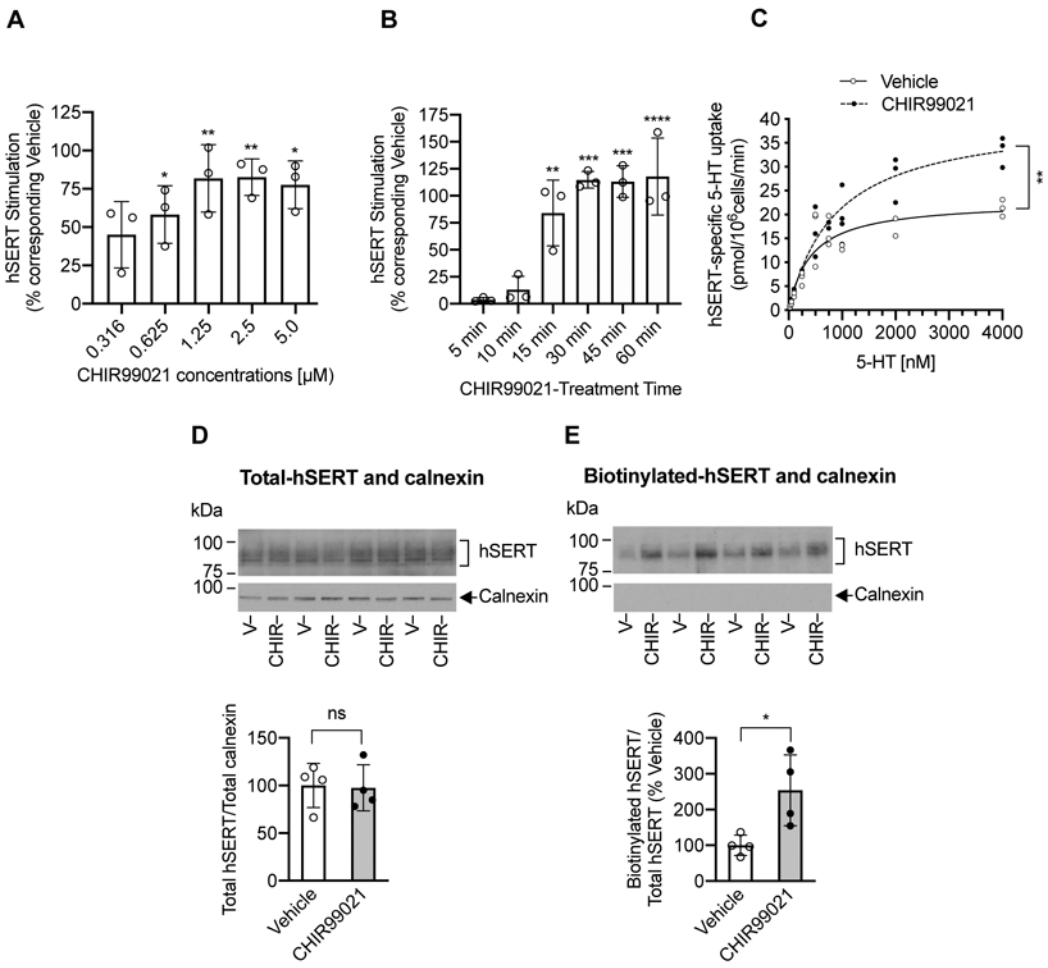

FIGURE 3. Effect of GSKα/ß inhibitor CHIR99021 on hSERT-mediated 5-HT uptake, hSERT kinetics, and hSERT surface expression in HEK-293 cells.

(A and **B).** Effect of CHIR99021 dose and treatment time on 5HT uptake. HEK-293 cells were transfected with hSERT-WT. After 24 h transfection, cells were preincubated at 37°C for 45 min with vehicle or various concentrations of CHIR99021 **(A)** or preincubated at 37°C with vehicle or CHIR99021 (2.5 μM) for various times **(B)**. Following preincubation, hSERT-specific [^{3}H]5-HT uptake was performed, and presented as percentage change of 5-HT uptake from the corresponding vehicle treated controls (mean ± SD). Vehicle-treated; N=3 and CHIR99021 treated; N=3 represents each independent cell culture preparations by averaging two or three replicates. **(A)**. CHIR99021 pretreatment stimulates hSERT activity in a dose-dependent manner (one-way ANOVA: $F_{(5.12)} = 6.589$, P =0.0036). Bonferroni's multiple comparison test: *P =0.0240 (0.625 μM), **P =0.0020 (1.25 μM), **P =0.0019 (2.5 μM), *P =0.0125 (5 μM) compared with vehicle. **(B)**. CHIR99021 stimulates SERT activity in a time-dependent manner (two-way ANOVA: time, $F_{(4,8)} = 15.13$, P =0.0008; treatment, $F_{(1,2)} = 175.9$, P =0.0056; time and treatment interaction ($F_{(4,8)} = 10.24$, P =0.0031). Bonferroni's multiple comparison test: **P =0.022 (15 min), *** P =0.0001 (30 min), ***P =0.0001 (45 min), ****P <0.0001 (60 min) compared with vehicle. **(C)**. Effect of CHIR99021 on hSERT kinetics in HEK-293 cells. HEK-293 cells expressing hSERT-WT were treated with vehicle or CHIR99021 (2.5 μM) for 45 min at 37°C. Following treatments,

hSERT specific [^{3}H]5-HT uptake was measured using various concentrations of 5-HT. Nonlinear curve fits of uptake data were shown. Each point represents data from one independent cell culture preparation performed in duplicates. **P =0.0096 (t-test, N=3 independent experiments) compared with vehicle. Due to very close values, some data points got merged. **(D** and **E)**. Effect of CHIR99021 on surface SERT. After 24 h post transfection of hSERT-WT, cells were treated with vehicle or CHIR99021 (2.5 μM) for 45 min at 37°C and cell surface biotinylation was performed. Representative immunoblots of four independent experiments show total **(D)** and biotinylated hSERT **(E)** as well as intracellular marker calnexin under each SERT respective immunoblot. Quantified total hSERT (~94-98 kDa) normalized to total calnexin (90 kDa) and quantified biotinylated hSERT normalized to total hSERT were shown under respective immunoblots (mean ± SD). CHIR99021 treated samples (N=4) are shown relative to vehicle-treated samples (N=4) samples and represent each independent cell culture preparations. Student's t-test: *P =0.0245 compared with vehicle, ns: non-significant effect (P =0.8879) compared with vehicle. V: Vehicle, CHIR: CHIR99021.

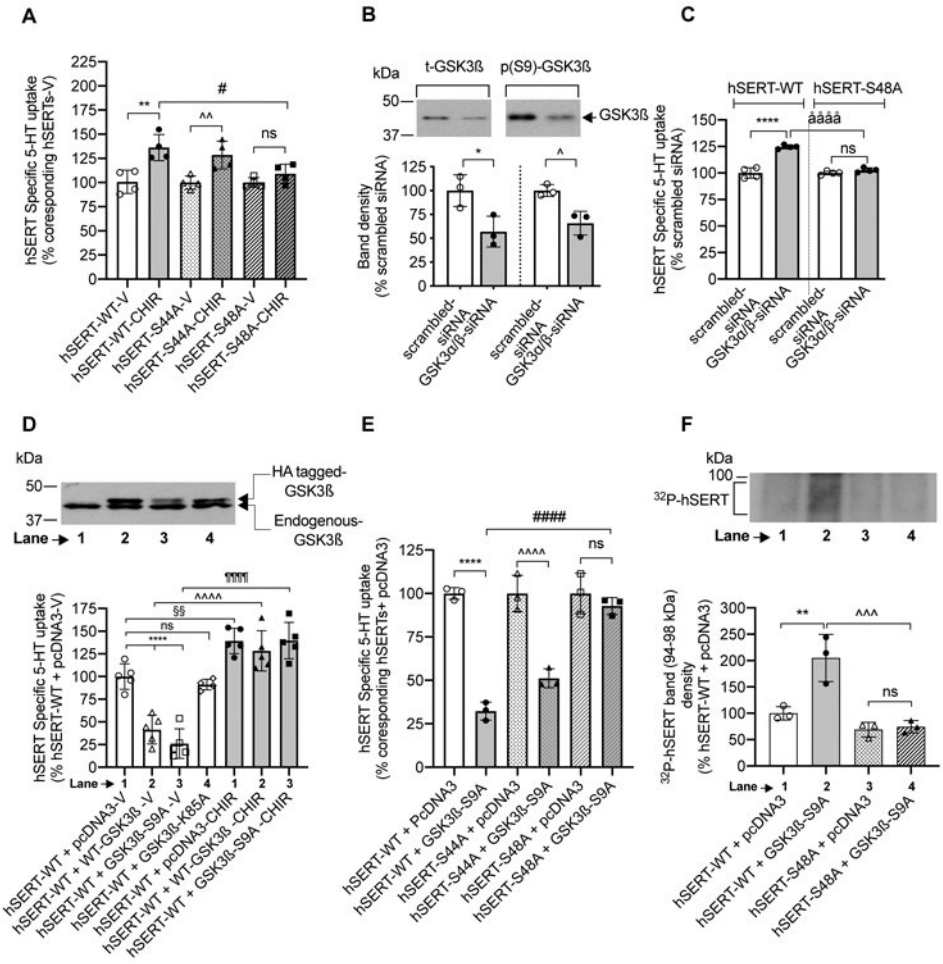

FIGURE 4. Effect of CHIR99021 and GSK3ß manipulations on the activity and phosphorylation of hSERT-WT and hSERT mutants (S44A and S48A).

(A). Effect of CHIR99021. HEK-293 cells were transfected with hSERT expression plasmids as indicated in the figure. After 24 h transfection, cells were incubated with vehicle or CHIR99021 (2.5 μM) for 45 min at 37°C and assayed for [^{3}H]5-HT uptake for 10 min at 37°C. Values are presented as percentage change of 5-HT uptake from corresponding vehicle treated controls. (one-way ANOVA: $F_{(5.18)} = 8.741$, P =0.0002). Bonferroni's multiple comparison test: **P =0.001 and ^^P =0.0077 compared with vehicle ns: no significant effect (P =0.1023) compared vehicle. $^{\#}$P =0.00116 compared with hSERT-WT. Each point in the graph represents one individual independent cell culture preparation by averaging two or three replicates (N=4, mean ± SD). **(B** and **C).** Effect of GSK3α/β knockdown. HEK-293 cells were transfected with hSERT-WT or hSERT-S48A plus GSK3α/β- siRNA or control scrambled siRNA. After 48 h transfection, expression levels of t-GSK3ß and (p(S9)- GSK3β), and [^{3}H]5-HT uptake were determined. **(B)**. Representative western blot shows the expression levels of t-GSK3ß and p(S9)- GSK3β. Band intensities are presented in the lower panel. *P =0.0401 and ^P =0.0387 compared with control scrambled siRNA (Paired Student's t-test, N=3 independent well each, mean ± SD). **(C)**. siRNA targeted to GSK3α/β stimulates SERT-WT activity, but no effect on hSERT-S48A activity (one-way ANOVA: $F_{(3,12)} = 66.94$, P <0.0001). Bonferroni's multiple comparison

test: N=4 independent experiments; ****P <0.0001, ååååP <0.0001 compared between specified pairs. ns. non-significant effect (P =0.6426) between specified pairs. Each data point represents one individual experiment by averaging two or three replicates. Due to very close values, some data points got merged. **(D, E** and **F)**. Effect of GSK3ß manipulations and the influence of CHIR99021 on hSERT activity and phosphorylation. hSERT-WT or hSERT-mutants were co-transfected with empty pcDNA3 vector (control) or with GSK3ß-constructs. After 24 h transfection, uptake of [^{3}H]5-HT or GSK3ß immunoblotting was performed. **(D).** Representative western blot image shows the expression of transfected HA-tagged GSK3β and endogenous GSK3β. Graph below the immunoblot shows the effect of co-expression of GSK3ß-WT, constitutively active GSK3ß (GSK3ß-S9A) or inactive GSK3ß (GSK3ß-K85A), and the influence of CHIR99021 on hSERT mediated 5-HT uptake. GSK3ß-WT and GSK3ß-S9A expression significantly decreased hSERT-WT activity following vehicle treatment (One-way ANOVA: ($F_{(6,27)}$ = 39.04, P <0.0001). Bonferroni's multiple comparison test: ****P <0.0001; §§P <0.0082; ^^^^P <0.0001; ¶¶¶¶P <0.0001 compared between specified pairs. ns: non-significant (P >0.9999) effect. Mean ± SD, N=5 independent cell culture preparations performed in duplicates or triplicates **(E)**. Graph shows the effect of active GSK3ß-S9A co-expression on the activity of hSERT-WT, hSERT-S44A and hSERT-S48A. GSK3ß-S9A co-expression significantly reduced hSERT-WT and hSERT-S44A activity, but not hSERT-S48A activity. (one-way ANOVA: $F_{(5.12)}$ = 47.78, P <0.0001). Bonferroni's multiple comparison test: ****P <0.0001, ^^^^P <0.0001 and ####P <0.0001 compared between specified pairs. ns: no significant effect (P >0.9999) between indicated pairs . Mean ± SD, N=3 independent cell culture preparations performed in triplicate. **(F)**. A representative autoradiogram of three independent experiments shows ^{32}P-labelled hSERT bands (~94-98 kDa). Quantified ^{32}P-labelled hSERT band densities from three independent experiments are shown (mean ± SD). Co-expression of active GSK3ß-S9A with hSERT-WT but not with hSERT-S48A increased ^{32}P-labelling of hSERT, (one-way ANOVA: $F_{(3,8)}$ = 19.31, P =0.0005). Bonferroni's multiple comparison test: **P =0.0035, ^^^P =0.0008 compared between indicated pairs. ns: non-significant (P >0.9999) effect between indicated pairs. V: Vehicle, CHIR: CHIR99021.

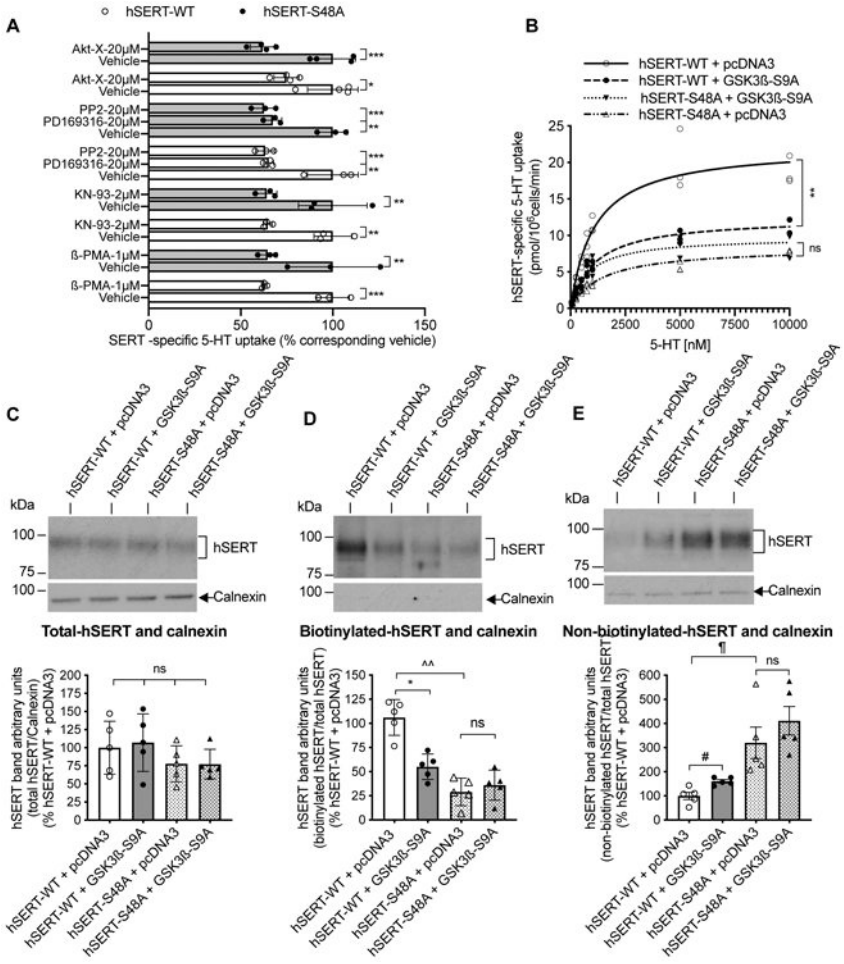

FIGURE 5. Effect of kinase modulators, and active GSK3ß co-expression on 5-HT transport, kinetics and surface expression of hSERT-WT and hSERT-S48A in HEK-293 cells.

(A). HEK-293 cells expressing hSERT-WT or hSERT-S48A were pretreated with indicated concentration of kinase modulators (Y-axis) for 30 min and [^{3}H]5-HT uptake was measured for 10 min at 37°C. Kinase modulators significantly decreased 5-HT uptake in both hSERT-WT and hSERT-S48A (one-way ANOVA: $F_{(17,40)} = 9.302$, P <0.0001). Bonferroni's multiple comparison test: *P =0.0138, **P =0.0014, 0.001, 0.0017, 0.0040, ***P =0.0007, 0.0008 compared with respective vehicle. Mean ± SD, N=3 independent cell culture preparations performed in triplicate. **(B)**. HEK-293 cells were co-transfected with hSERT-WT + pcDNA3 or hSERT-WT + GSK3ß-S9A or hSERT-S48A + pcDNA3 or hSERT-S48A + GSK3ß-S9A. After 24 h transfection, hSERT specific 5-HT uptake was measured using various concentrations of 5-HT. Nonlinear curve fits of uptake data were shown from (N=3); each data point represents an individual independent cell culture preparation by averaging two or three replicates. Due to very close values, some data points got merged. Co-expression of GSK3ß-S9A significantly decreased V_{max} of hSERT-WT and had no effect on the V_{max} of hSERT-S48A (two-way repeated measures (RM) ANOVA: interactions: $F_{(1,4)} = 44.02$, P =0.0027, pcDNA3 vs GSK3ß-S9A: $F_{(1,4)} = 22.50$, P =0.0090, hSERT-WT vs hSERT-S48A: $F_{(1,4)} = 90.15$, P =0.04823). Bonferroni's multiple comparison test: **P =0.0020 compared between hSERT-WT + GSK3ß-S9A and hSERT-WT + pcDNA3. ns. non-

significant (P =0.5070) compared between hSERT-S48A + GSK3ß-S9A and hSERT-S48A + pcDNA3. **(C-E)**. Representative immunoblots of independent cell culture preparations show total hSERT **(C)**, biotinylated surface hSERT **(D)**, and non-biotinylated intracellular hSERT **(E)**. Intracellular marker calnexin from total extract, biotinylated and non-biotinylated fractions are also shown under each respective SERT immunoblot. Quantified bands densities (~94-98 kDa) of total hSERT normalized to total calnexin (90 kDa), biotinylated hSERT normalized to total hSERT, and non-biotinylated hSERT normalized to total hSERT are presented under respective immunoblots. *P =0.0198, ^^P =0.0044, #P =0.0423, ¶P =0.0428 compared between specified pairs. ns: non-significant effect between indicated pairs (paired Student's t-test, N=5, mean ± SD).

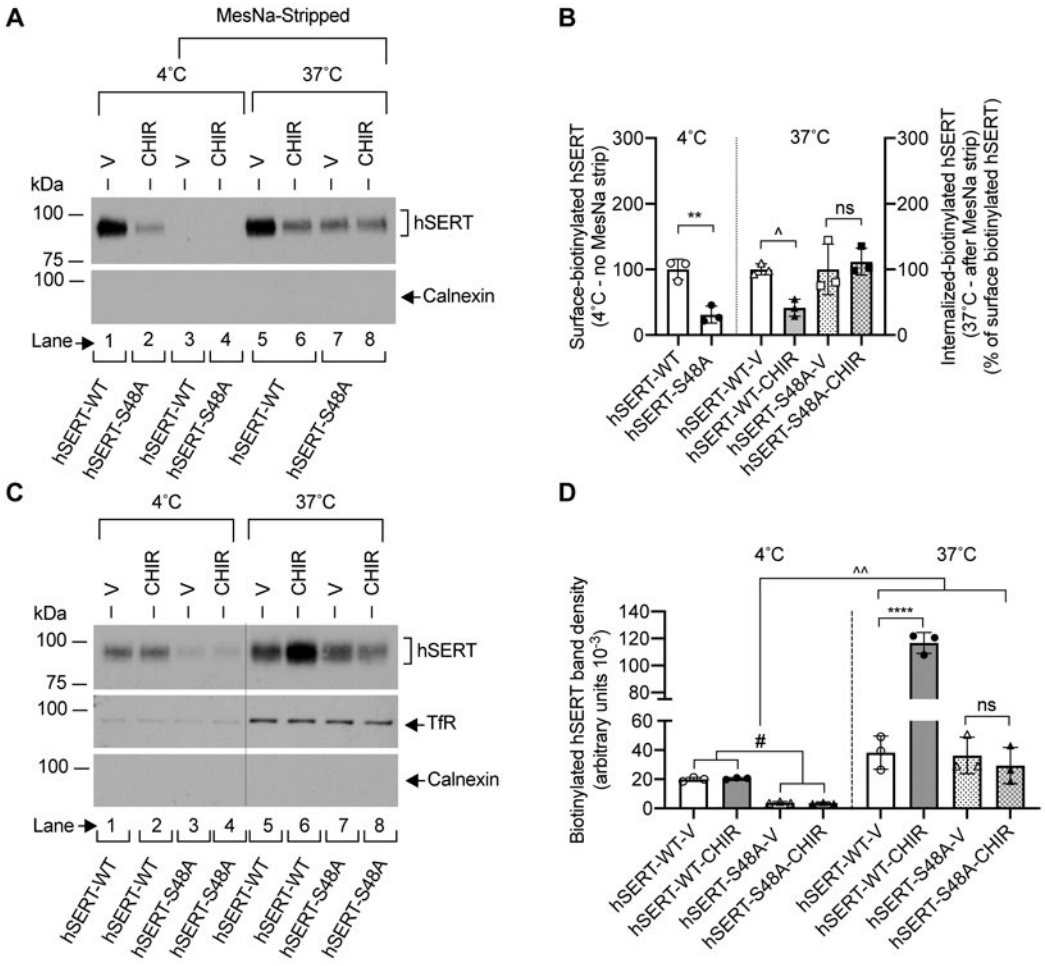

FIGURE 6. Effect of CHIR99021 on the internalization and plasma membrane insertion of hSERT-WT and hSERT-S48A in HEK-293 cells.

(A). Representative immunoblot of three independent experiments shows the surface-biotinylated hSERT before (lanes 1 and 2) and after MesNa treatment (lanes 3 and 4) (4°C), and internalized-biotinylated hSERT (37°C) after MesNa treatment (lanes 5, 6, 7 and 8). Intracellular marker calnexin from biotinylated fractions is also shown. **(B)**. Quantified band densities (N=3 independent cell culture preparations, mean ± SD) of biotinylated hSERT bands (~94-98 kDa) reveal that CHIR99021 (2.5 μM) treatment for 30 min at 37°C significantly decreased hSERT-WT internalization, but had no effect on hSERT-S48A internalization (one-way ANOVA: $F_{(5,21)} = 8.581$, P =0.0012). Bonferroni's multiple comparison test: **P =0.0045, ^P =0.0138 compared between specified pairs. ns. non-significant (P =0.999) effect between indicated pairs. **(C)**. HEK-293 cells expressing hSERT-WT or hSERT-S48A were incubated with biotinylating agent at 4°C (lanes 1, 2, 3 and 4) or 37°C (lanes 5, 6, 7 and 8) with vehicle or CHIR99021 (2.5 μM) for 30 min to biotinylate cell surface proteins. Calnexin and TfR levels were visualized following stripping the blots and reprobing with calnexin and TfR antibodies, and shown under hSERT immunoblot (**C**). Excised lanes 1, 2, 3 and 4 (4°C) from the same immunoblot were indicated with a vertical dashed line. A representative immunoblot of three independent experiments is shown. (**D**). Quantified biotinylated hSERT bands (N=3 independent cell culture preparations, mean ±

SD) show that CHIR99021 treatment significantly enhanced hSERT-WT plasma membrane insertion, but had no effect on hSERT-S48A plasma membrane insertion (one-way ANOVA: $F_{(7,16)} = 61.85$, P =0.0001). Bonferroni's multiple comparison test: ****P <0.0001, ^^P =0.0014, #P =0.0115 compared between specified pairs. ns. non-significant (P =0.999) effect between indicated pairs. V: Vehicle, CHIR: CHIR99021, TfR: Transferrin Receptor.